

UC San Diego

UC San Diego Previously Published Works

Title

Polygenic networks in peripheral leukocytes indicate patterns associated with HIV infection and context-dependent effects of cannabis use

Permalink

<https://escholarship.org/uc/item/4rn6p82b>

Authors

Basova, Liana V

Lukkes, Savannah Eve

Milner, Richard

et al.

Publication Date

2022-03-01

DOI

10.1016/j.bbih.2022.100414

Peer reviewed



## Polygenic networks in peripheral leukocytes indicate patterns associated with HIV infection and context-dependent effects of cannabis use



Liana V. Basova<sup>a</sup>, Savannah Eve Lukkes<sup>b</sup>, Richard Milner<sup>a</sup>, Ronald J. Ellis<sup>c</sup>, Mariana Cherner<sup>c</sup>, Jennifer Iudicello<sup>c, \*\*</sup>, Maria Cecilia Garibaldi Marcondes<sup>a, \*</sup>

<sup>a</sup> San Diego Biomedical Research Institute, San Diego, CA, 92121, USA

<sup>b</sup> National Institute of Drug Abuse Summer Intern, 2021, USA

<sup>c</sup> Department of Psychiatry, University of California San Diego, San Diego, CA, 92093, USA

### ARTICLE INFO

#### Keywords:

Cannabis  
HIV  
Biomarker  
Inflammation  
Cognition

### ABSTRACT

In spite of suppressive antiretroviral therapies (ART), Human Immunodeficiency Virus (HIV)-infected subjects still experience the consequences of viral persistence and chronic inflammation. In the brain, where most HIV-1 targets are of innate immune origin, neurological and cognitive impairments are detectable and enhanced by highly prevalent substance use disorders. Cannabis is one of the most prevalent substances among HIV+ subjects, compared to non-infected populations, either prescribed for improving various symptoms or used recreationally, as well as a component of polysubstance use. The mechanisms by which addictive substances and HIV interact are multifactorial and poorly understood. Importantly, the HIV brain target cells, macrophages and microglia, express receptors to neurotransmitters elevated by such drugs, and express receptors to cannabinoids, particularly CB2R. We have tested a panel of 784 transcripts associated with neurological disorders, digitally multiplexed and detectable in peripheral blood cells from a small cohort (n = 102) of HIV-positive (HIV+) and HIV-negative (HIV-) specimens, stratified based on criteria of lifetime (LT) dependence of cannabis (CAN+) or not (CAN-). Demographic homogeneity and low incidence of co-morbidities helped increase power and allowed the identification of key differences consistent with HIV infection, cannabis exposure, or their interactions. A small percentage of these subjects used cannabis as well as other drugs. The data was analyzed using robust systems and visualization strategies to detect orchestrated patterns in gene networks connected based on molecular interfaces with higher power than in single genes. We found that the effects of cannabis differed drastically between HIV- and HIV+ groups, particularly in gene networks playing a role in inflammation, neurodegeneration, apoptosis and leukocyte adhesion and transmigration. At the level of individual genes, we identified detrimental effects that were associated with polysubstance use as a covariate, particularly methamphetamine. Transcription factor usage predictions suggest that the effects of cannabis are associated with transcriptional co-regulation at the gene promoters by multiple factors that vary by context. Overall, we have found that the effects of cannabis may be context-dependent, with potential benefits in the context of HIV reflected by improvements in cognition, but in the absence of the polysubstance use component.

### 1. Introduction

Under suppressive antiretroviral therapies (ART), infection with Human Immunodeficiency Virus (HIV) remains a challenge, both due to the maintenance of cellular reservoirs and to chronic inflammation driven by low viral replication and dysregulated immune mechanisms (Wong et al., 2019; Bachmann et al., 2019; Yuan and Kaul, 2021; Hunt et al., 2016). In end organs such as the brain, where the majority of the

HIV-1 targets and reservoirs are of myeloid origin (Wallet et al., 2019; Gama et al., 2017; Veenstra et al., 2017), the remaining inflammatory environment contributes to co-morbidities (Zicari et al., 2019), including neurological and cognitive problems (Brew and Barnes, 2019; Saloner et al., 2021; Heaton et al., 2015), particularly if ART is not introduced sufficiently early (Marcondes et al., 2009). Substance use disorders (SUD) are frequent among the HIV-infected population, further contributing to cognitive impairment (Byrd et al., 2011; Brew and McArthur, 2019;

\* Corresponding author. 3525 John Hopkins Court, #200, 92121, San Diego, CA, USA.

\*\* Corresponding author. 9500 Gilman Dr. MC0041, La Jolla, CA, 92093, USA.

E-mail addresses: [jiudicello@health.ucsd.edu](mailto:jiudicello@health.ucsd.edu) (J. Iudicello), [cmarcondes@SDBRI.org](mailto:cmarcondes@SDBRI.org) (M.C.G. Marcondes).

<https://doi.org/10.1016/j.bbih.2022.100414>

Received 11 October 2021; Received in revised form 17 December 2021; Accepted 10 January 2022

Available online 15 January 2022

2666-3546/© 2022 The Authors. Published by Elsevier Inc. This is an open access article under the CC BY-NC-ND license (<http://creativecommons.org/licenses/by-nc-nd/4.0/>).

**Table 1**  
Cohort demographic, health and psychiatric characteristics.

N	HIV-/CAN-		HIV+/CAN-		HIV-/CAN+		HIV+/CAN+		P value
	Mean	STD	Mean	STD	Mean	STD	Mean	STD	
Age	36.57	7.72	37.75	7.14	37.36	10.88	37.32	6.36	0.95
Education	13.25	2.62	13.12	2.81	13.14	2.25	12.22	2.67	0.37
Global T score	46.97	6.75	45.52	5.74	48.91	5.26	47.02	6.73	0.055
CD4 Nadir	889.7	214.2	263.11**	194.15	835.61	172.99	345.59**	275.98	<0.0001
CD4/CD8 Ratio	2.13	1.25	0.54**	0.33	2.05	1.41	0.56**	0.29	<0.0001
% Black	6		0		4		3		-
% Hispanic	4		10		3		1		-
% Asian	0		1		1		1		-
% White	18		17		14		16		-
Detectable Plasma VL (N)			17**				12**		0.028
Detectable CSF VL (N)			17**				10**		0.0123
LT METH dep (N)	13		13		12		12		0.34
LT Alcohol dep (n)	13		12		20*		12*		0.013
LT Cocaine dep (N)	4		4		10*		10*		0.015
LT Opioid dep (N)	1		1		6*		3*		0.031
LT MDD (N)	8		16**		8		14**		0.0259

STD = standard deviation, VL= Viral Load; dep = dependence, LT = lifetime, METH = methamphetamine, MDD = major depressive disorder, \*p < 0.05 CAN+/CAN- in multiple comparisons, \*\*p < 0.05 HIV+/HIV- in multiple comparisons.

**Table 2**  
Domains collected in Standardized Neuropsychological Test Battery.

Domain	Assessment
Premorbid Intellectual Functioning	Wide Range Achievement Test (WRAT-IV) Reading Subtest
7 Neurocognitive Ability Domains	Standardized Neurocognitive Tests
Verbal Fluency	Controlled Oral Word Association Test – Letter Fluency (F-A-S) Category Fluency (Animals) Action/Verb Fluency (“Things people do”)
Abstraction/Executive Functioning	Wisconsin Card Sorting Test (WCST) Trail Making Test – Part B Stroop Color and Word Test – Interference score Halstead Category Test
Attention/Working Memory	Wechsler Adult Intelligence Scale (WAIS)-III Letter-Number Sequencing Wechsler Memory Scale (WMS)-III Spatial Span Subtest Paced Auditory Serial Addition Task (PASAT)
Learning (Verbal/Visual)	Hopkins Verbal Learning Test-Revised (HVLT-R) – Total Learning Brief Visuospatial Memory Test-Revised (BVMTR) – Total Learning
Memory (Verbal/Visual)	Hopkins Verbal Learning Test-Revised (HVLT-R) – Delayed Recall Brief Visuospatial Memory Test-Revised (BVMTR) – Delayed Recall
Speed of Information Processing	Wechsler Adult Intelligence Scale (WAIS)-III/IV Digit Symbol Subtest Wechsler Adult Intelligence Scale (WAIS)-III/IV Symbol Search Subtest Trail Making Test – Part A Stroop Color Word Test – Color Naming
Motor	Grooved Pegboard Test

Paolillo et al., 2020). Nonetheless, the mechanisms by which addictive substances and HIV interact are multifactorial and poorly understood. Drugs of abuse impact the brain reward system, by modifying levels and balance of neurotransmitters (Koob and Volkow, 2016; Volkow and Morales, 2015). The HIV target cells, macrophages and microglia, as well as CD4 T cells, express receptors to neurotransmitters, so SUDs are likely to impact mechanisms of immune and inflammatory, and anti-viral responses (Magrone and Jirillo, 2019; Burdo et al., 2006; Ferris et al., 2008). Biomarkers that detect the effect of SUDs, and distinguish HIV in that context, may clarify how drugs affect HIV and inflammation.

Cannabis is one of the most prevalent substances among HIV+ subjects, compared to the non-infected population (Watson et al., 2020), either prescribed for ameliorating symptoms associated with the virus or with ART (Whiting et al., 2015), or used recreationally, as well as a component of polysubstance use (Gonzalez et al., 2004), which in itself is a risk factor for HIV infection. The effects of cannabis may drastically differ from the effects of stimulant drugs such as Methamphetamine (METH), particularly in the context of HIV infection (Saloner et al., 2020). Yet, similar to other drugs of abuse, cannabis may be a confounder shifting the expression of biomarkers of inflammation and cognition, masking our ability to clearly measure the impact of virus, ART or other treatments in the immune status and brain pathogenesis, or may be altogether beneficial.

In terms of cognition, cannabis exposure has been linked to lower odds of impairment in people living with HIV (Watson et al., 2020). On the other hand, impaired verbal learning and memory, may be negatively impacted by cannabis use (Grant et al., 2003). Other studies report no differences, or detrimental effects in HIV-negative populations, suggesting that the observed effects of cannabis, including its benefits, may be largely domain and context-dependent.

It has been reported that cannabis use improves biomarkers of inflammation in the CSF and plasma of HIV+ subjects (Ellis et al., 2020) and decreases the number of circulating inflammatory cells (Rizzo et al., 2018). We have tested the value of a large panel of transcripts associated with inflammation and neurological disorders, digitally multiplexed and detectable in peripheral blood cells from HIV-positive (HIV+) and HIV-negative (HIV-) subjects, users of cannabis (CAN+) or not (CAN-). The differences between groups were analyzed using a systems biology approach that identified associated gene networks based on pathways and molecular interfaces, for identifying and visualizing orchestrated transcriptional patterns consistent with HIV infection, CAN exposure, and their interactions. Trends in the behaviors of gene clusters and their predicted regulators revealed that effects of cannabis differ between HIV- and HIV+ groups. Moreover, mixed statistical models have pinpointed genes that are further influenced by cannabis in the context of polysubstance use. These context-dependent effects of cannabis indicate the complexity of its molecular actions and properties, and the challenges of biomarker discovery in the context of SUDs. At the same time, the results suggest that cannabis in the context of HIV infection may drive benefits by promoting a decrease of pro-inflammatory and neurotoxic transcriptional patterns, changes and changes in gene clusters associated with leukocyte transmigration and neurological disorders.

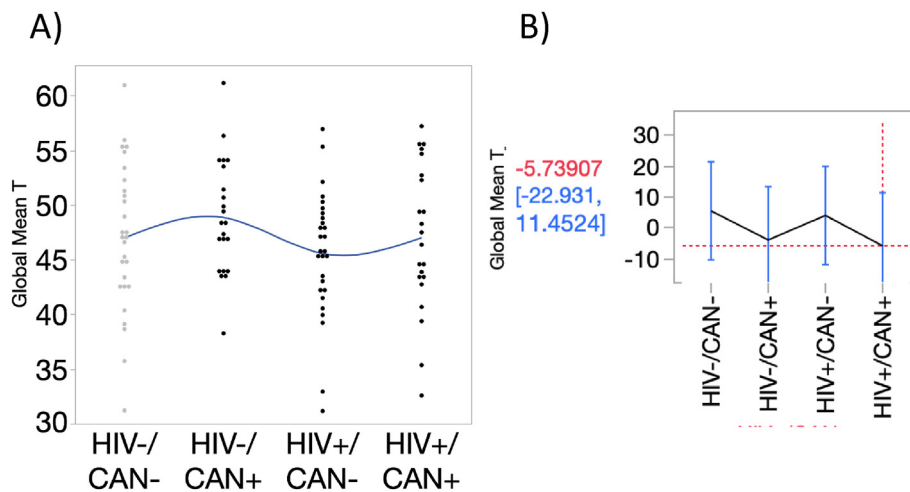


Fig. 1. Effect of cannabis on Global T scores. A) Individual Global Mean T scores per group. B) Marginal Model Profiler of Cannabis effects on Global T-score.

## 2. Material and methods

### 2.1. Cohort

Participants included 102 adults enrolled by the University of California San Diego's HIV Neurobehavioral Research Center (HNRC) and Translational Methamphetamine Research Center (TMARC) under informed consent and approved protocols. Neurocognitive testing was conducted using previously described protocols (Carey et al., 2004; Blackstone et al., 2012). Peripheral blood leukocytes were collected during visits and archived. The subjects selected to this study were males, between 35 and 49 years old, divided based on HIV status (HIV+/-) and on Cannabis use (CAN+/-). CAN+ was defined as met lifetime DSM-IV criteria for cannabis abuse or dependence. A cross-sectional design assembled the following groups: HIV-CAN- (n = 28), HIV+CAN- (n = 23), HIV-CAN+ (n = 28) and HIV+CAN+ (n = 23). Exclusion criteria was history of non-HIV-related neurological, medical or psychiatric disorders that affect brain function (e.g., schizophrenia, traumatic brain injury, epilepsy), learning disabilities, or dementia. Major depressive disorder (MDD) and polysubstance use, including lifetime (LT) methamphetamine (METH), opioid and alcohol dependence were not excluded given the prevalence of these conditions in the populations examined and occurred in about 50% of the HIV+ subjects. Table 1 shows the characteristics of the cohort, including values of health and psychiatric assessment.

### 2.2. Neurocognitive (NC) assessment

The NC assessment included a measure of premorbid verbal IQ (Wide Range Achievement Test-4 – Reading subtest) and measures assessing seven ability domains commonly affected by CNS dysfunction associated with HIV and substance use, including speeded information processing, learning, memory, verbal fluency, executive functions, attention/working memory, and motor skills. Tests included in the NC battery were standardized, well-validated, and reliable, with appropriate normative data available (Heaton and Taylor, 2004; Heaton and Manly, 2002; Norman et al., 2011), and included (listed by domain): (1) Learning: Total Learning Trials 1–3 from the Hopkins Verbal Learning Test – Revised (HVLT-R) and the Brief Visuospatial Memory Test – Revised (BVMT-R); (2) Memory: HVLT-R and BVMT-R Delayed Recall; (3) Attention/Working Memory: Paced Auditory Serial Addition Task (PASAT)-50 item, Wechsler Memory Scale (WMS)-III Spatial Span subtest, and the Wechsler Adult Intelligence Scale (WAIS)-III Letter Number Sequencing subtest; (4) Executive Functions: Wisconsin Card Sorting Test (WCST), Trail Making Test- Part B, Halstead Category Test, and the

Stroop Color Word Test-interference subtest; (5) Speeded Information Processing (SIP): Stroop Color Word Test-color naming subtest; WAIS-III Digit Symbol subtest, WAIS-III Symbol Search subtest; (6) Verbal Fluency: Controlled Oral Word Association Test (COWAT-FAS), Animal Fluency, and Action Fluency; and (6) Fine motor skills: Grooved Pegboard test (dominant and nondominant hand total scores). Raw scores from each test were converted to demographically-corrected standard scores (T-scores) using the best available normative standards which correct for effects of age, education, sex, and ethnicity, as appropriate (Norman et al., 2011) (Heaton and Taylor, 2004; Heaton and Manly, 2002) and were averaged within each domain to obtain NC domain T-scores, which were then averaged to obtain the Global T-score which was used for analyses (Table 2).

### 2.3. Peripheral leukocytes specimens

Archived specimens were thawed in fetal bovine serum, washed and viability was counted using disposable hemocytometers (Bulldog Bio, Portsmouth, NH). Cell numbers were adjusted for flow cytometry and for RNA extraction. All specimens were number-coded and experimenters were blinded.

### 2.4. Flow cytometry

Washed cells with adjusted concentrations of 105/100 $\mu$ l were resuspended in HBSS without phenol red, containing 2% fetal bovine serum and 0.2% sodium azide, and stained with pre-defined concentrations of subset, function and activation-specific antibodies. The antibodies used in staining were: CD11b, CD14, CD16, CD38, CCR5, ICAM1, PDL1, CD49d, CX3CR1, MRP8/14 and RAGE. Following incubation, cells were washed and resuspended in 4% Paraformaldehyde. Tubes were kept at 4 °C and protected from light until acquisition. Cell acquisition was performed in a CytoFlex S benchtop platform (Beckman Coulter, Indianapolis, IN), and analyzed using FlowJo software (FlowJo LLC, Ashland, OR).

### 2.5. RNA extraction

The RNA purification from pellets was performed using Nucleospin RNA Mini kit with DNA separation column (Macherey-Nagel, Bethlehem, PA). RNA quality and levels were monitored in a NanoDrop spectrophotometer ND-2000 (Thermo Scientific, Waltham, MA), and used to adjust concentrations for subsequent assays.

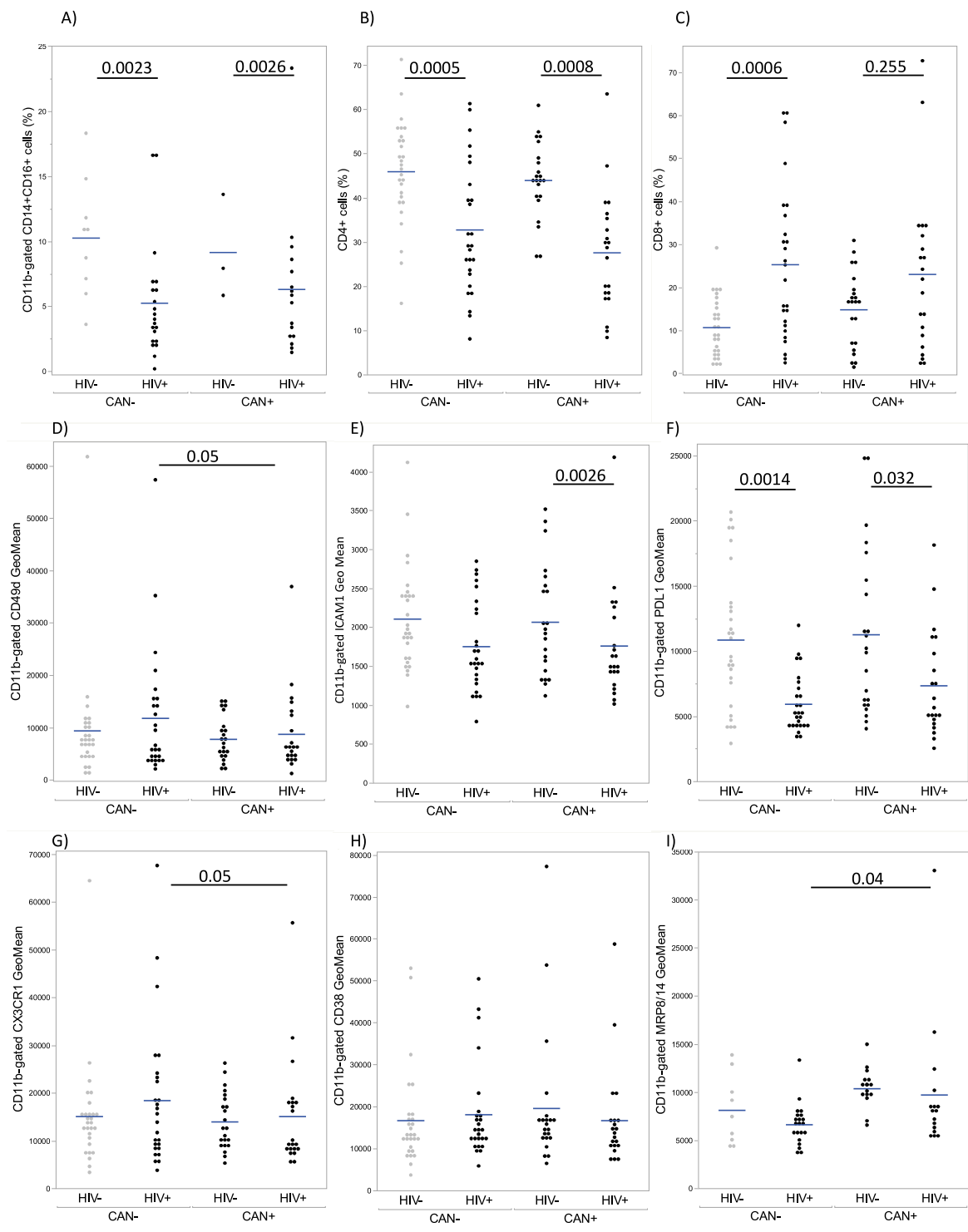


**Fig. 2.** Percentages of peripheral blood cell subsets measured by flow cytometry, and geometric mean fluorescence of markers involved in leukocyte transmigration and activation status. A) Percentage of CD11b+ CD14+ CD16+ monocytes. B) Percentage of CD4+ T cells. C) Percentage of CD8+ T cells. D) Geometric mean fluorescence (GeoMean) of CD49d on the surface of gated CD11b+ monocytes. E) GeoMean fluorescence of ICAM-1 on gated CD11b+ monocytes. F) GeoMean of PDL1 on gated CD11b+ monocytes. G) GeoMean of CX3CR1 on gated CD11b+ cells. H) GeoMean of MRP8/14 on gated CD11b+ cells. Individual values are represented as scatter plots, with marked average and standard deviations. The p values of group comparisons are indicated in the figure.

## 2.6. Digital multiplex gene expression assays

The nCounter gene expression assays (NanoString Technologies, Seattle, WA) were performed using a custom-made combination of Neuropathology and Neuroinflammation NanoString panels. Briefly, panel code-set probes were hybridized with 150 ng of total RNA per

specimen over 18hr at 65 °C in a SimplyAmp Thermocycler (Applied Biosystems, Waltham, MA), according to manufacturer's protocol. Hybridized RNA was then diluted in molecular grade water and loaded into nCounter SPRINT cartridge (NanoString) in nCounter SPRINT Profiler, and then RNA-conjugated probes were counted via NanoString SPRINT Profiler technology. Results from each panel were merged into one data

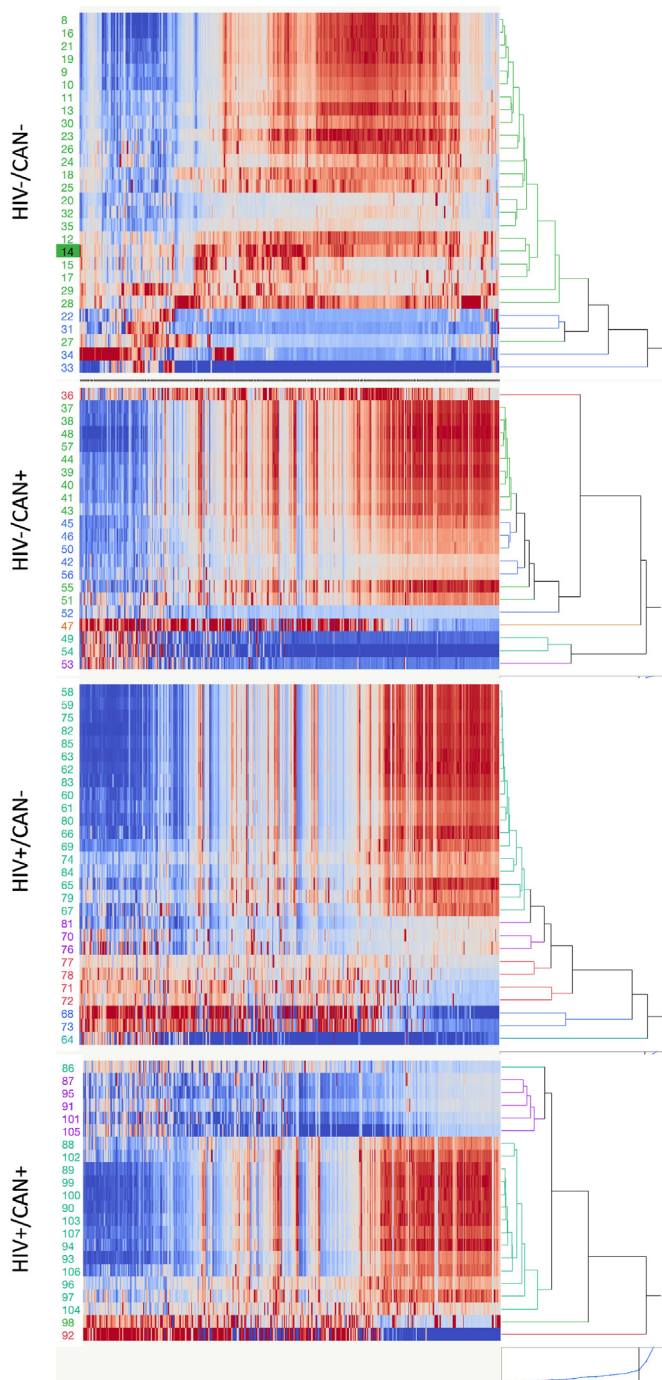


**Fig. 3. Hierarchical subject x gene clustering based on average expression patterns.** Two-way hierarchical clustering was performed in all normalized expression data and visualized by group using distance scale. The order of the genes in the X-axis was constant in all four panels for comparison. Upper panel shows HIV-/CAN-, followed by HIV-/CAN+, HIV+/CAN- and HIV+/CAN+.

file for comparative analysis. Reference gene normalization was performed for each sample by dividing each sample's raw count profiles by the geometric mean of 8 reference genes in nSolver, as previously described (Danaher et al., 2017). Genes that did not show signal in any specimen were excluded from subsequent systems analysis.

## 2.7. Statistical analysis

Scores were calculated as the log<sub>2</sub> normalized expression of each

gene. Variance due to noise for each score was estimated in a linear mixed model. Pairwise comparisons and false discovery rate were calculated for each group. Fitted value models were used to determine variable and intercept effects. Multiple comparisons were performed using Tukey HD. Predictor screening was used to determine specific effects of individual variables, named HIV and Cannabis, and their interaction. Mixed models were used to identify interactive effects of polysubstance use (methamphetamine, alcohol, opioids), detectable cerebrospinal fluid (CSF) viral load, and Global T-score on gene expression. All statistical analysis was performed in JMP Pro 15.2.0 software (SAS Institute Inc., Cary, NC, USA).

## 2.8. Systems analysis and visualization tools

Processes and pathway annotations were performed in DAVID Bioinformatics Resources 6.8 (<https://david.ncicfcrf.gov>, 2020) and visualized using local search features in GeneMANIA plugin (Franz et al., 2018; Montojo et al., 2010, 2014a, 2014b; Warde-Farley et al., 2010) ([www.genemania.org](http://www.genemania.org)) in Cytoscape 3.7.0 platform (Shannon et al., 2003) ([www.cytoscape.org](http://www.cytoscape.org), 2020) with *Homo sapiens* sources from Reactome (Haw et al., 2011; Stein, 2004) ([www.reactome.org](http://www.reactome.org), 2020) and BioGRID\_ORGANISM (Oughtred et al., 2021; Stark et al., 2006) (<https://thebiogrid.org>, 2020). Transcription factor-DNA interactions derived from merged peak regions were modeled using licensed TRANSFAC v2021.1 and iRegulon in Cytoscape 3.7.0, as previously described (Basova et al., 2021; Tjitro et al., 2018).

## 3. Results

### 3.1. Cohort characteristics and cell surface markers

The impact of HIV, cannabis and their interaction on peripheral markers of cell subset, cellular function and activation was estimated using a combination of cell surface protein detection by flow cytometry and a targeted digital multiplex transcriptomic analysis. The specimens were from males, with homogeneous age and education, and the same race distribution, as shown in Table 1. The examination of clinical data revealed that in HIV+ individuals, cannabis did not significantly affect CD4 nadir, CD4/CD8 ratio, plasma or CSF viral load. Cannabis users were significantly more likely to engage in polysubstance use, or use other drugs, including alcohol, cocaine and METH. HIV status significantly increased the incidence of lifetime major depressive disorders, which was not affected by cannabis use (Table 1). Neuropsychological data indicated that cannabis had a marginal effect on Global T scores (Table 1, Table 2 and Fig. 1).

By flow cytometry, we verified that the specimen freezing process did not impact subset distribution (Lucy et al., 1988). For instance, HIV+ subjects had significantly lower percentage of CD11b<sup>+</sup>CD14<sup>+</sup> monocytes compared to HIV- subjects, particularly the ones exhibiting the inflammatory marker CD16<sup>+</sup>, regardless of cannabis use (Fig. 2A). The percentage of CD4<sup>+</sup> T cells was also decreased in HIV+ specimens when compared to HIV-, with no effect of cannabis (Fig. 2B). The percentage of CD8<sup>+</sup> cells, on the other hand, was significantly increased in HIV+ non-cannabis users, but not in cannabis users, compared to respective controls (Fig. 2C).

### 3.2. Gene expression patterns and gene interactions

Molecular markers of neuroinflammation, activation and leukocyte transmigration were measured in the peripheral blood cells under the hypothesis that cannabis use has an effect by itself and on modulating the effects of HIV. A panel of 784 markers relevant to neurological disorders and inflammation were tested by Nanostring. Of these 381 did not produce any signal in any of the specimens and were excluded from the analysis. The expression of genes with significant signal over noise in more than arbitrarily 10% of the samples was normalized by an average

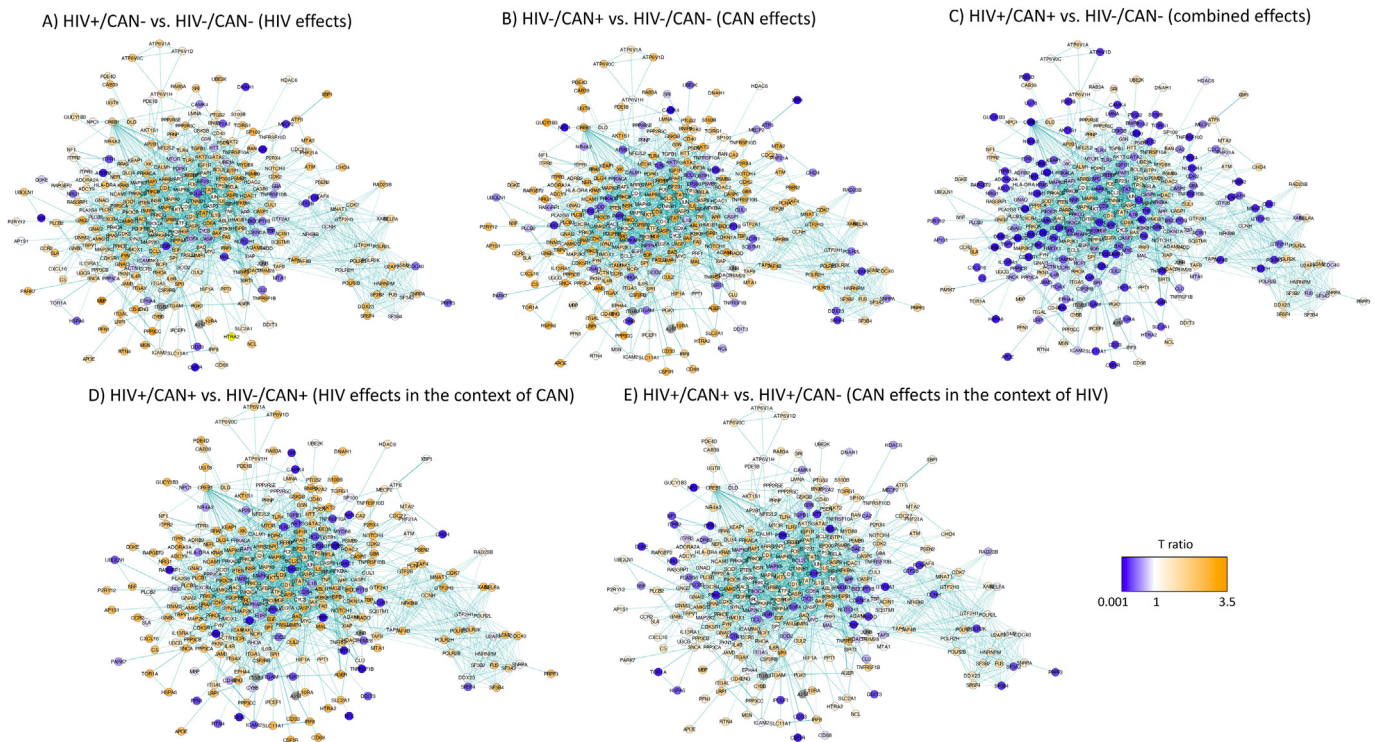


**Fig. 4. Genes connected by pathway.** Blue lines indicate pathway-based interactions. Node colors represent the ratio between the average of groups, as indicated. Genes that are decreased in comparisons are indicated by shades of blue. Genes that are increased in comparisons are indicated in shades of orange. No change is represented in white. Cut off ratio was 1.5-fold. A) The effects of HIV alone were estimated by the ratio of HIV+/CAN- versus (vs.) HIV-/CAN-, with 189/305 genes in orange (increase above 1.5 ratio) and 33/305 in blue (below 1.5 ratio). B) The effects of cannabis alone were estimated by HIV-/CAN+ vs. HIV-/CAN-, 196/305 genes in orange and 46/305 in blue. C) The combined effects were estimated by the ratio between HIV+/CAN+ vs. HIV-/CAN-, with 55/305 genes in orange and 133/305 in blue. D) The effects of HIV in the context of cannabis were measured by HIV-/CAN+ vs. HIV+/CAN+, with 182/305 genes in orange and 47/305 in blue. E) The effects of cannabis in the context of HIV were detected by the ratio between HIV+/CAN- vs. HIV+/CAN+, with 127/305 genes in orange and 51/305 in blue. (For interpretation of the references to color in this figure legend, the reader is referred to the Web version of this article.)

of 8 housekeeping genes. Hierarchical clustering performed using average normalization method applied to digital gene expression data has revealed similarities between HIV-/CAN+, HIV+/CAN- and HIV+/CAN+, but all these groups were distinct from HIV-/CAN-. Clustering also allowed to identify individual specimens that showed patterns distinct from the majority within groups (Fig. 3).

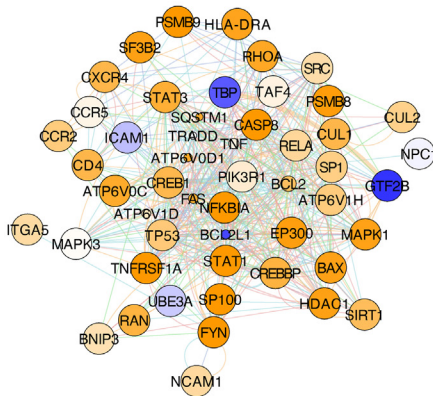
Systems biology strategies were used to identify defining expression patterns in transcriptional data, and gene clusters exhibiting orchestrated behaviors perturbed by HIV infection, by the use of cannabis, or by their interaction. We have identified significant trends in a number of gene clusters functionally annotated to biological processes and pathways of relevance to the neuropathogenesis of HIV. Overall, the analysis indicates context-dependent effects of cannabis.

The majority of the digitally multiplexed genes (305 genes) exhibited detectable and overlapping interactions based on pathway, as indicated in Fig. 4. The effects of HIV alone were estimated by the ratio comparison between HIV+/CAN- versus (vs.) HIV-/CAN-. The effects of cannabis alone were estimated by the ratio between HIV-/CAN+ vs. HIV-/CAN-. The overall combined effects were estimated by the ratio between HIV+/CAN+ vs. HIV-/CAN-. The effects of HIV in the context of cannabis were measured by the ratio between HIV-/CAN+ vs. HIV+/CAN+. The effects of cannabis in the context of HIV were detected by the ratio between HIV+/CAN- vs. HIV+/CAN+. The visual inspection of the cluster in Fig. 4 shows that both HIV and cannabis alone increase the expression of a number of genes indicated by nodes with orange color (Fig. 4A and 4B, respectively). In cells from HIV+/CAN+ individuals, a number of genes showed decreased expression compared to HIV-/CAN- (Fig. 4C). HIV infection in the context of cannabis, revealed by the comparison of HIV+/CAN+ and HIV-/CAN+ (Fig. 4D), was characterized by stronger upregulation of genes, but also several genes with decreased expression.

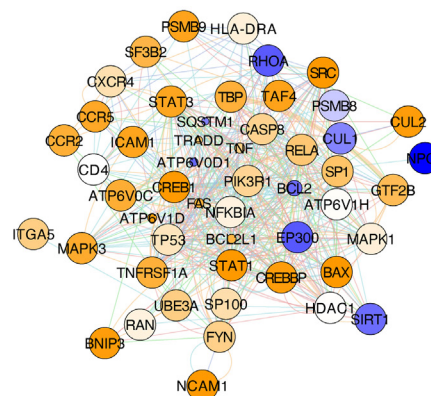
The effects of cannabis in the context of HIV (Fig. 4E) measured by the ratio between HIV+/CAN+ and HIV+/CAN-, were characterized by a higher number of downregulated genes, and a more modest upregulation, as suggested by overall lighter orange shades. A complete list of the genes in this network and T ratio in indicated comparisons can be found in Supplementary Materials 1.

Pathway-based interactions were subdivided for identification of embedded functional annotations impacted by HIV and/or cannabis, identified by DAVID Bioinformatics Resources with a gene list input. Individual functional annotations were then assembled in GeneMania for visualization of effects. A complete list of significant pathways and functional annotations can be found in Supplementary Materials 1. The pathways selected for visualization were curated based on the expression of inflammatory genes, significance to neurological disorders in the context of HIV, viral infection, pathogenesis and networks with interventional value. For instance, a gene network functionally annotated to viral host interactions was identified (Fig. 5), where the ratio between HIV+/CAN- and HIV-/CAN- (Fig. 5A) indicated that HIV increased a number of genes annotated to that function. The ratio between HIV-/CAN+ and HIV-/CAN- (Fig. 5B), as well as between HIV+/CAN+ subjects were compared to HIV-/CAN+ (Fig. 5C), indicated that both cannabis alone and HIV in the context of cannabis use increased a large number of genes in this cluster, but several genes were also decreased in both conditions, including the Ras homolog gene family GTPase RhoA, the Proteasome 20S Subunit Beta 8 (PSMB8), the intracellular cholesterol transporter (NPC1), the E1A Binding Protein P300 (EP300) and the histone deacetylase Sirtuin 1 (SIRT1). The ratio between HIV+/CAN+ and HIV+/CAN- indicated that cannabis in the context of HIV was associated with a mild increase of genes in viral host interaction function (Fig. 5D), and a decrease in the general transcription factor IIB (GTF2B)

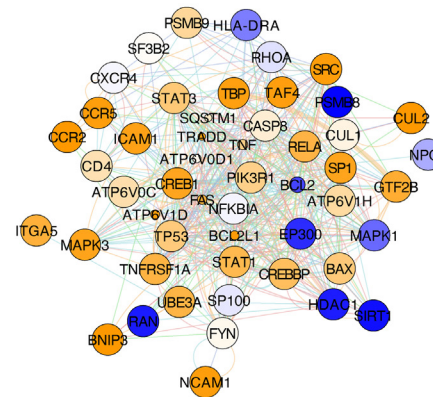
A) HIV+/CAN- vs. HIV-/CAN-



B) HIV-/CAN+ vs. HIV-/CAN-



C) HIV-/CAN+ vs. HIV+/CAN+



D) HIV+/CAN- vs. HIV+/CAN+

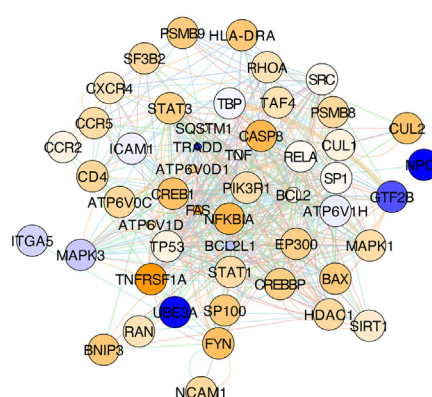
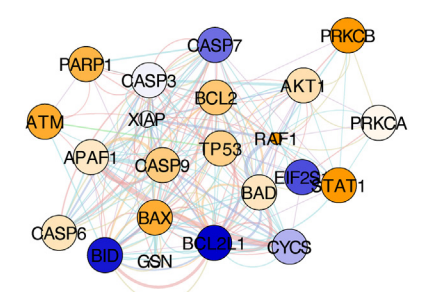
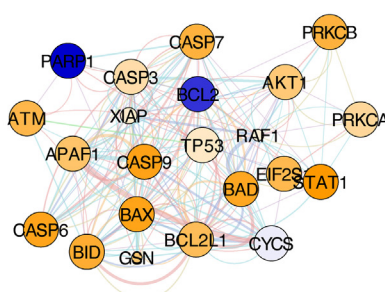


**Fig. 5. Viral host interaction.** Viral host interaction functional annotation derived from pathway interactions were identified. Fold enrichment = 8.75, Benjamini  $p = 5.79E-33$ , FDR  $p = 1.01E-33$ . Connectors indicate pathway (green, 9.44% weight), co-localization (blue, 7.2% weight) and physical interactions (light pink, 36.74% weight). Node colors represent the ratio between the average of groups, as indicated. Genes that are decreased in T ratio comparisons are indicated by shades of blue. Genes that are increased in comparisons are indicated in shades of orange. No change is represented in white. (For interpretation of the references to color in this figure legend, the reader is referred to the Web version of this article.)

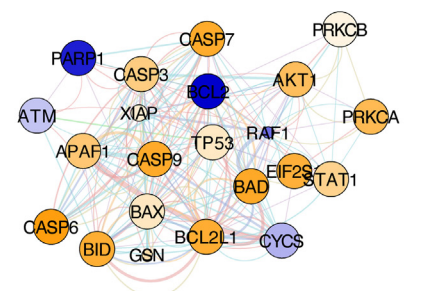
A) HIV+/CAN- vs. HIV-/CAN-



B) HIV-/CAN+ vs. HIV-/CAN-



C) HIV+/CAN+ vs. HIV-/CAN+



D) HIV+/CAN+ vs. HIV+/CAN-

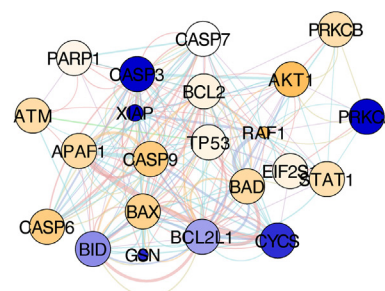


**Fig. 6. Apoptosis.** Apoptosis functional annotation derived from pathway interactions were identified. Fold enrichment = 12.98, Benjamini  $p = 6.73E-27$ , FDR  $p = 2.35E-27$ . Connectors indicate pathway (green, 24.63% weight), co-localization (blue, 11.32% weight) and physical interactions (light pink, 35% weight). Node colors represent the ratio between the average of groups, as indicated. Genes that are decreased in T ratio comparisons are indicated by shades of blue. Genes that are increased in comparisons are indicated in shades of orange. No change is represented in white. (For interpretation of the references to color in this figure legend, the reader is referred to the Web version of this article.)



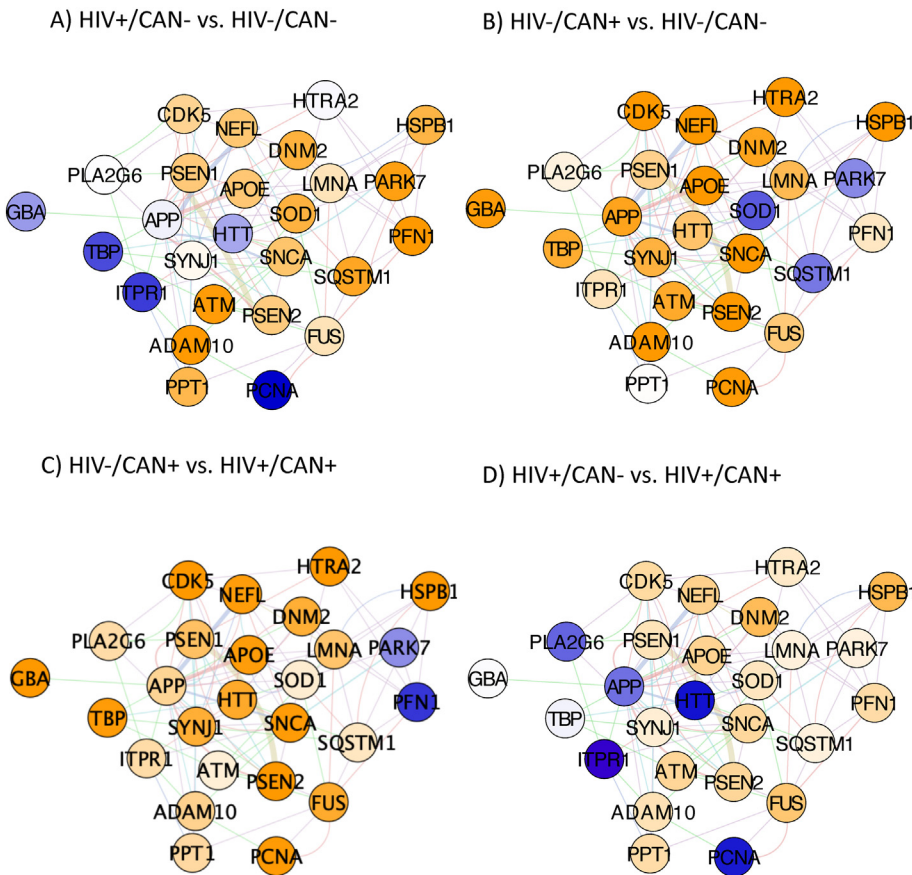


**Fig. 7. Neurodegeneration and inflammation.** Merged neurodegeneration and Inflammation functional annotations were derived from pathway interactions. Fold enrichment for neurodegeneration = 5.22, Benjamini  $p = 9.76 \cdot 10^{-4}$ , FDR  $p = 9.98 \cdot 10^{-6}$ . Fold enrichment for inflammation = 6.47, Benjamini  $p = 1.36 \cdot 10^{-11}$ , FDR  $p = 9.33 \cdot 10^{-14}$ . Connectors indicate pathway (green, 37.77% weight), co-localization (blue, 1.01% weight), predicted interactions (light orange, 2.34%) and physical interactions (light pink, 19.09% weight). Node colors represent the ratio between the average of groups, as indicated. Genes that are decreased in T ratio comparisons are indicated by shades of blue. Genes that are increased in comparisons are indicated in shades of orange. No change is shown in white. (For interpretation of the references to color in this figure legend, the reader is referred to the Web version of this article.)

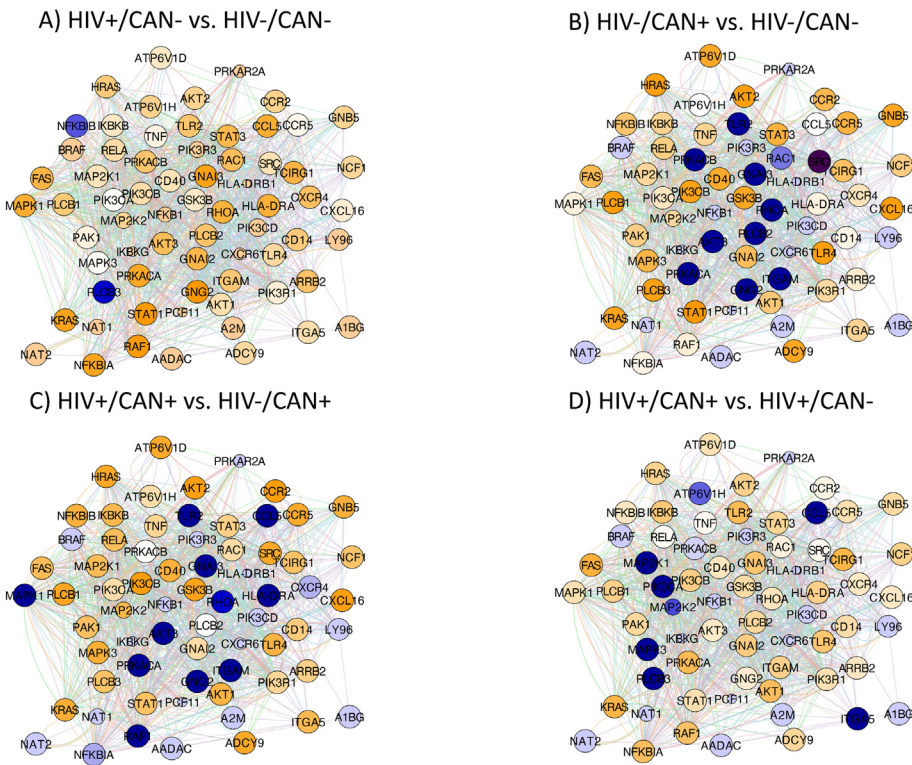


**Fig. 8. Chemokines and Cytokines.** Chemokines and cytokines functional annotations derived from pathway interactions were identified. Fold enrichment = 2.86, Benjamini  $p = 2.38 \cdot 10^{-4}$ , FDR  $p = 1.35 \cdot 10^{-4}$ . Connectors indicate pathway (green, 37.04% weight), co-localization (blue, 2.78% weight), predicted interactions (light orange, 17.37%) and physical interactions (light pink, 26.97% weight). Node colors represent the ratio between the average of groups, as indicated. Genes that are decreased in T ratio comparisons are indicated by shades of blue. Genes that are increased in comparisons are indicated in shades of orange. No change is represented in white. (For interpretation of the references to color in this figure legend, the reader is referred to the Web version of this article.)

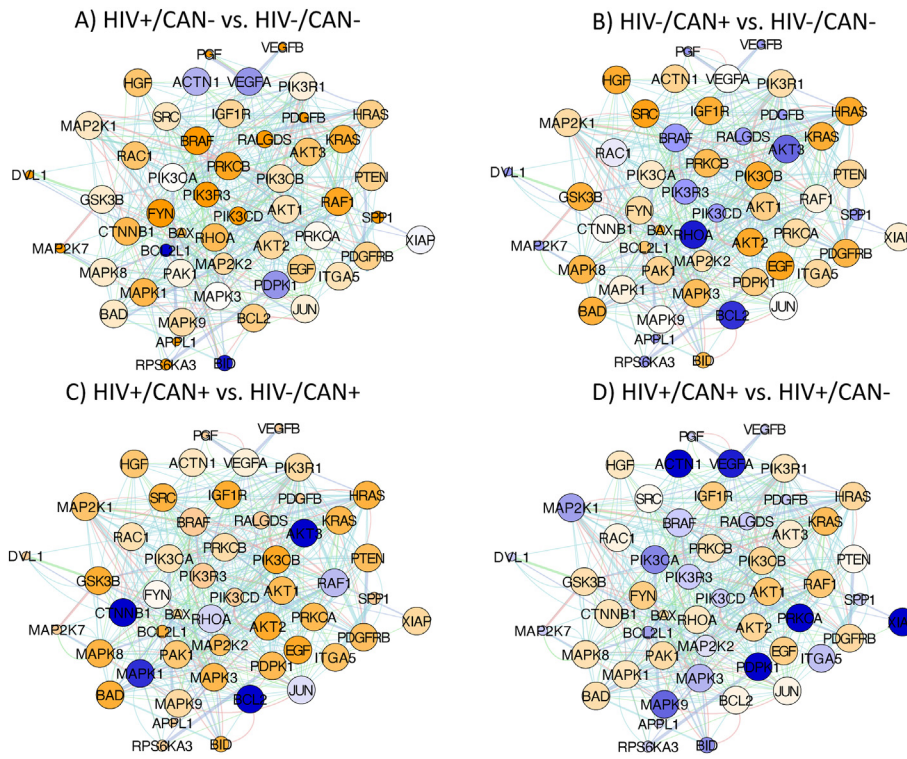


**Fig. 9. Vascular adhesion and leukocyte transmigration.** Focal adhesion, Vascular Endothelial Growth Factor (VEGF) - signaling and leukocyte transmigration functional annotations were derived from pathway interactions and merged for visualization due to high overlap (83%). Fold enrichment = 10.39, Benjamini  $p = 3.24 \cdot 10^{-17}$ , FDR  $p = 5.16 \cdot 10^{-19}$ . Connectors indicate pathway (green, 10.98% weight), co-localization (blue, 5.52% weight), predicted interactions (light orange, 18.92%), and physical interactions (light pink, 23.38% weight). Node colors represent the ratio between the average of groups, as indicated. Genes that are decreased in T ratio comparisons are indicated by shades of blue. Genes that are increased in comparisons are indicated in shades of orange. No change is represented in white. (For interpretation of the references to color in this figure legend, the reader is referred to the Web version of this article.)

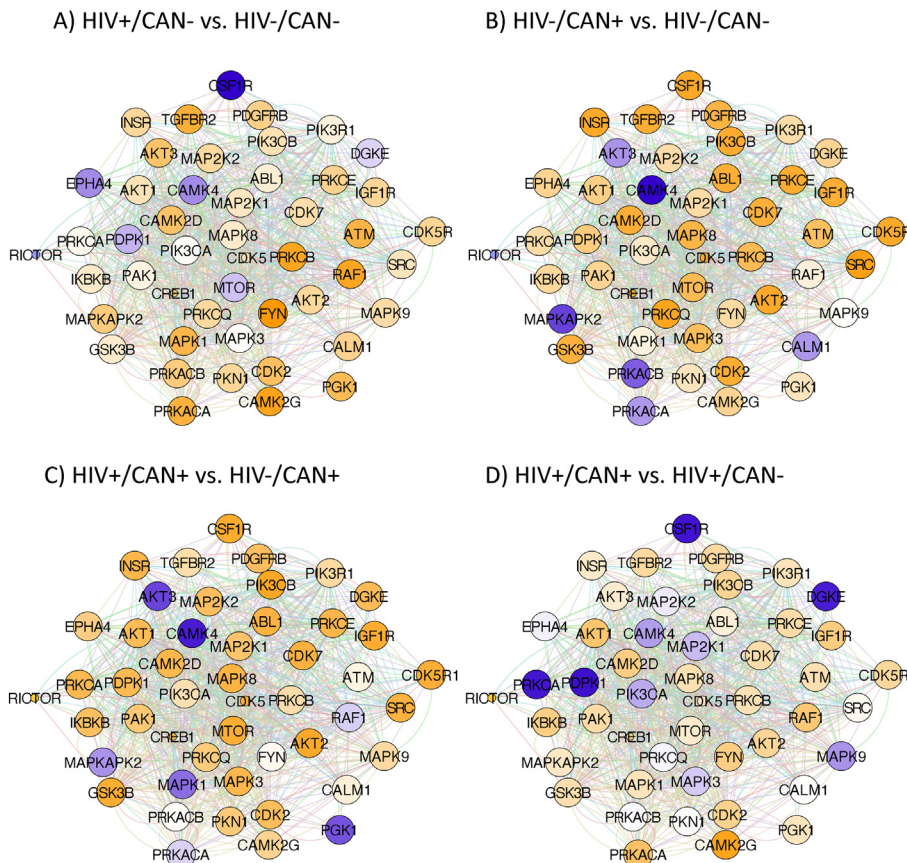


**Fig. 10. Kinases.** Kinase functional annotations were derived from pathway interactions. Fold enrichment = 7.14, Benjamini  $p = 1.47 \cdot 10^{-7}$ , FDR  $p = 1.89 \cdot 10^{-9}$ . Connectors indicate pathway (green, 37.77% weight), co-localization (blue, 1.01% weight), predicted interactions (light orange, 2.34%) and physical interactions (light pink, 19.09% weight). Node colors represent the ratio between the average of groups, as indicated. Genes that are decreased in T ratio comparisons are indicated by shades of blue. Genes that are increased in comparisons are indicated in shades of orange. No change is represented in white. (For interpretation of the references to color in this figure legend, the reader is referred to the Web version of this article.)

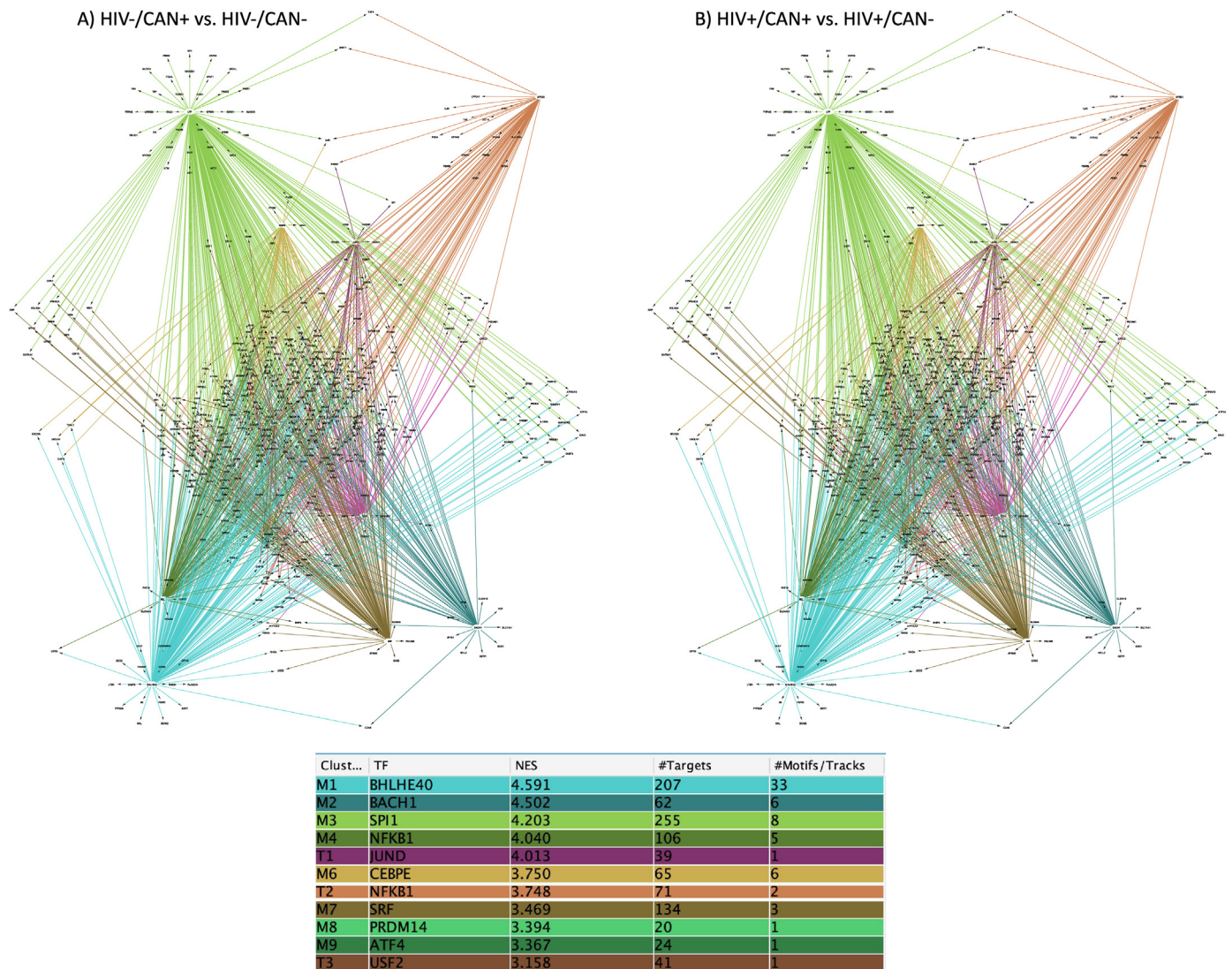


**Fig. 11. Mapping of transcription factor usage in pathway interactions associated with cannabis expression patterns in uninfected and HIV+ subjects.** Transcription factor regulation of genes connected by pathway was predicted using iRegulon in Cytoscape. Clusters were identified by connectors, color coded to identify transcription factors. The lower panel table shows the transcription factors, number of binding motifs (NES), number of target genes in the network, and average number of binding motifs in promoters. Node colors represent the ratio between the average of groups, as indicated. Genes that are decreased in T ratio comparisons are indicated by shades of blue. Genes that are increased in comparisons are indicated in shades of orange. No change is represented in white. Blue nodes represent the predicted transcription factors. (For interpretation of the references to color in this figure legend, the reader is referred to the Web version of this article.)

and the ubiquitin protein ligase 3A (UBE3A) were characteristic of this comparison.

Apoptosis was also identified as a relevant functional annotation (Fig. 6), showing differential effects of HIV and/or cannabis. HIV alone (visualized by the ratio between HIV+/CAN- and HIV-/CAN-) decreased Caspase 7 CASP7, but increased CASP9 and the apoptosis regulator BCL2 (Fig. 6A). The effect of cannabis, on the other hand (visualized by the ratio between HIV-/CAN+ and HIV-/CAN-), indicated decrease in BCL2 (Fig. 6B). Likewise, HIV in the context of cannabis (in the ratio between HIV+/CAN+ and HIV-/CAN+) had a decrease in BCL2 (Fig. 6C). On the other hand, the ratio between HIV+/CAN+ and HIV+/CAN- indicated that cannabis decreased or had mild effects on the expression of genes associated with apoptotic functions detectable in peripheral leukocytes (Fig. 6D).

Neurodegeneration and inflammation were functional annotations identified in BIOCARTA. Given the large degree of overlap between these networks (82%), we applied a merge network function in Cytoscape, which is shown in Fig. 7. The visualization of this gene network indicates that both HIV and cannabis increase genes with functions in

neurodegeneration and inflammation (Fig. 7A and 7B, respectively), but cannabis decreased key contributors to the inflammatory process such as IL1b, TLR2, MyD88 and PARK7, as well as RASGRP1 (Fig. 7B). HIV infection in the context of cannabis (Fig. 7C) indicated patterns that were similar to cannabis alone, with decreased expression in the same genes. Moreover, cannabis in the context of HIV elevated TLR2, TLR4 and MyD88, but had no or mild effects, or decreased a number of genes in this network (Fig. 7D).

Another gene network related to neurodegeneration and inflammation in Fig. 6 but low overlap (12%) and smaller but significant enrichment (2.86, FDR  $p = 1.35E-04$ ), was functionally annotated to chemokines and cytokines (Fig. 8). This network was highly sensitive to all the group conditions, with higher expression of most genes in cells from HIV+/CAN- compared with HIV-/CAN- (Fig. 8A), and an effect of cannabis that was characterized by decreased expression of several genes, regardless of HIV (Fig. 8B, 8C and 8D). Yet, the genes decreased by cannabis differed in a context-dependent manner. For instance, the effects of cannabis alone (Fig. 8B) as well as of HIV in the context of cannabis (Fig. 8C) showed a lower expression of TLR2, GNAI3, AKT3,

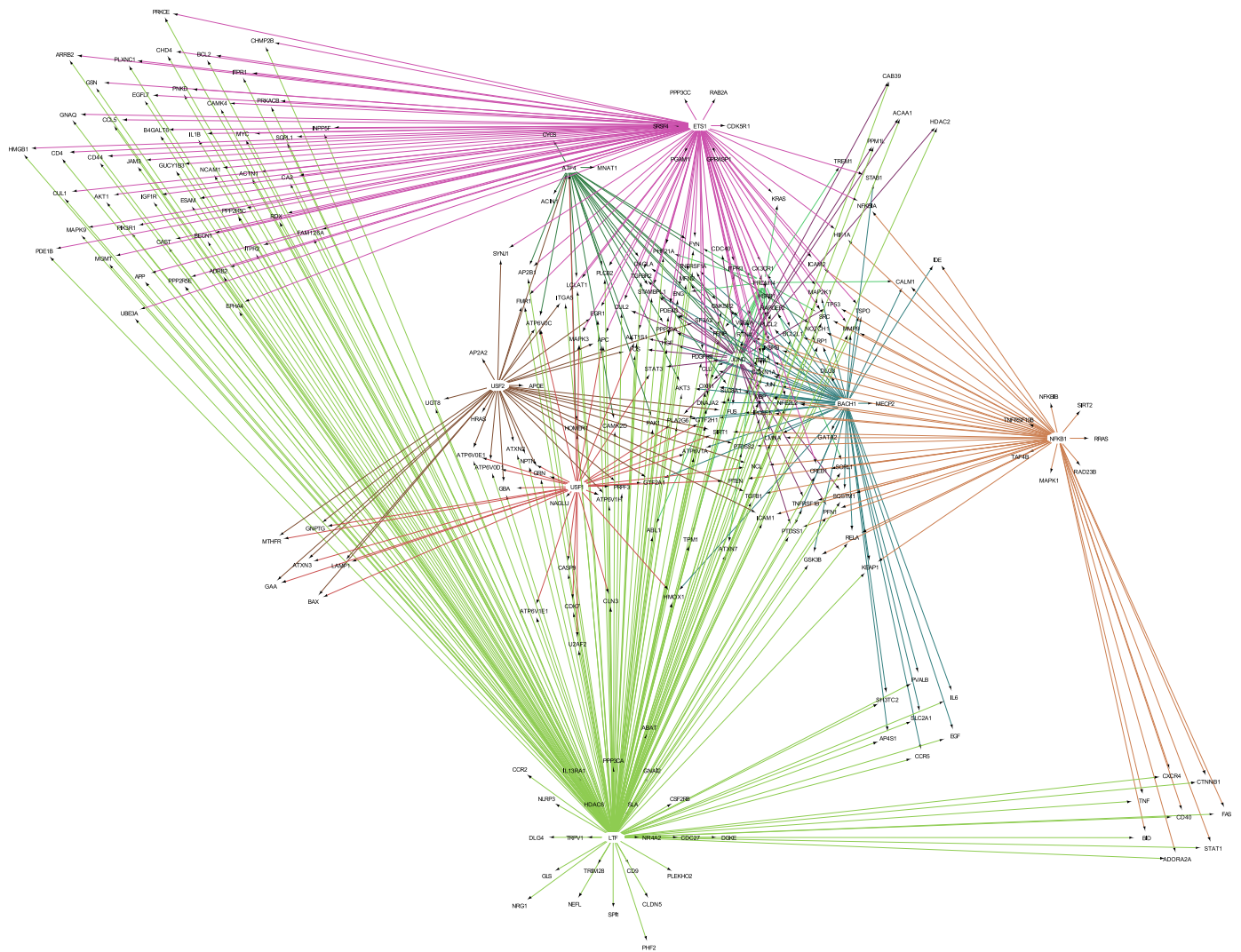


**Fig. 12. Co-regulated gene network and effects of cannabis in the context of HIV.** Node colors represent the ratio between the average of groups, as indicated. Genes that are decreased in T ratio comparisons are indicated by shades of blue. Genes that are increased in comparisons are indicated in shades of orange. No change is represented in white. Blue nodes represent the predicted transcription factors. (For interpretation of the references to color in this figure legend, the reader is referred to the Web version of this article.)

PRKACA, ITGAM, and GNG2, and a mild decrease of A1BG, Ly96, PIK3CD, BRAF, NAT1, NAT2, PRKAR2A and AADAC. Decrease in PLCB2 and RAC1 was a characteristic of cannabis alone (Fig. 8B), while decrease in RAF1 and NFKBIA was characteristic of HIV in the context of cannabis (Fig. 8C). The effects of cannabis in the context of HIV was also characterized by lower expression of MAPK3, PLCB3, CXCR6 and NFKB1 (Fig. 8D).

Functional annotations associated with leukocyte-vascular adhesion and transmigration capacity were also sorted from pathway interactions. These functions were affected by HIV and cannabis (Fig. 9). A large number of genes in this network were differentially increased by HIV and by cannabis (Fig. 9A and 9B, respectively). Yet cannabis lowered the expression of a large number of genes with cytoskeleton and signaling properties, including RHOA, AKT3, RAC1, BRAF and BCL2 (Fig. 9B). HIV in the context of cannabis had also lower MAPK1 and CTNNB1 compared to uninfected cannabis users (Fig. 9C). HIV+ cannabis users had a high number of genes that were lower or mildly changed compared to HIV non-cannabis users (Fig. 9D).

Inflammation is highly regulated by a kinases. HIV and cannabis affected the expression of a number of kinases and genes involved in kinase regulation. The effects were differential and context-dependent. All the conditions showed decrease in CAMK4, in comparison to

respective controls (Fig. 10). HIV alone decreased mTOR, CSF1R, EPHA4, PDPK1 and DGKE (Fig. 10A). Cannabis alone, as well as HIV in the context of cannabis (Fig. 10B and 10C, respectively), decreased ATK3 and MAPKPK2. Cannabis alone decreased CALM1 (Fig. 10B). HIV in the context of cannabis decreased the expression of PGK1 and RAF1 (Fig. 10C). Cannabis in the context of HIV decreased several genes in this network that were either not modified or increased by the other conditions (Fig. 10D). These included MAP2K1, MAPK9, MAPK3, PRKCA and PDPK1 (Fig. 10D).

### 3.3. Transcriptional regulation of cannabis patterns

Networks analyzed above have shown distinct effects of cannabis, which differed between cannabis alone and in the context of HIV. We used iRegulon to make predictions on transcription factors usage associated with these context-dependent patterns, in order to identify regulatory and co-regulatory elements. Fig. 11 shows the same gene network assembled based on pathway interactions in Fig. 3, but now reorganized based on the expression of transcription factor motifs in these genes' promoters.

The table legend in Fig. 11 shows the transcription factors mostly associated with the genes in the network. We have identified a significant

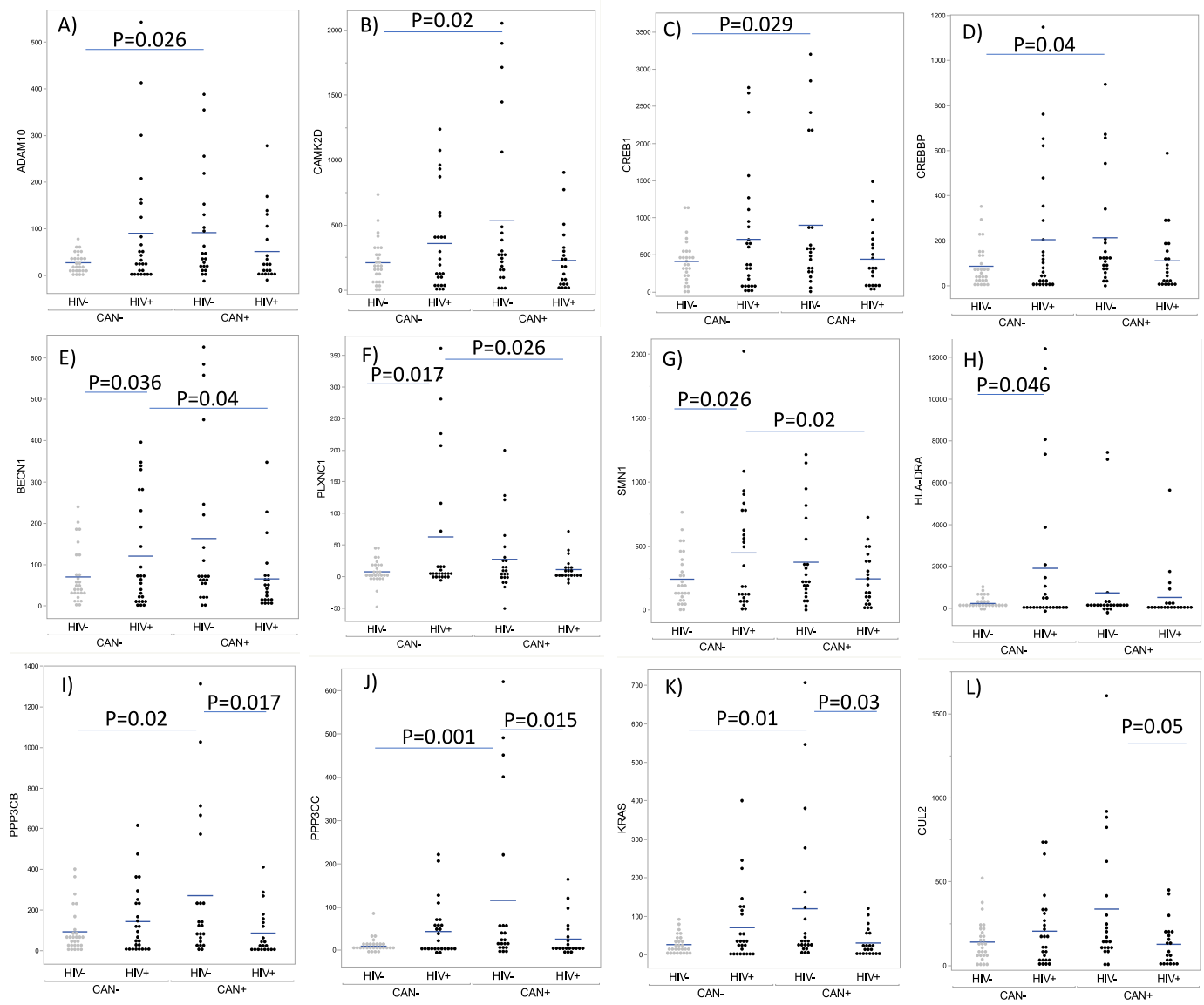


**Fig. 13. HIV and cannabis predictors.** Predictor screening functions were used to identify the genes that were most likely to indicate HIV or cannabis use, and HIV in the context of cannabis. The genes with significant predictor power are shown. Predictors were A) ADAM10, B) CAMK2D, C) CREB1, D) CREBBP, E) BECN1, F) PLXNC1, G) SMN1, H) HLA-DRA, I) PPP3CB, J) PPP3CC, K) KRAS and L) CUL2. Multiple comparisons using Tukey has indicated significance between groups, as shown by lines and by p values.

number of binding motifs to BHLHE40, BACH1, SPI1, NFKB1 (2), JUND, CEBPE, SRF, PRDM14, ATF4 and USF2. Mapping of genes regulated by these factors have revealed sub-clusters characterized by co-regulation. Interestingly, the visualization of effects of cannabis alone (Fig. 11A) and of cannabis in the context of HIV (Fig. 11B) suggests that the genes most affected by cannabis in the HIV+ subjects are more likely to be co-regulated by at least two transcription factors. A closer visualization of these genes is shown in Fig. 12, mapping the majority of the blue genes (showing decrease in HIV+/CAN+ compared to HIV+/CAN-, to NFKB1, BACH1, JUND and ETS1 regulation.

### 3.4. Predictors of cannabis, HIV and their interactions

Predictor screening was performed to identify markers that were most likely associated with individual groups, and that showed significant effects of HIV or cannabis. Twelve genes with biomarker potential have been found in peripheral leukocytes (Fig. 12). Of these, four genes were

predictors of uninfected cannabis users: a disintegrin and metalloproteinase domain-containing protein 10 (ADAM10, Fig. 13A), the Calcium/Calmodulin Dependent Protein Kinase II Delta (CAMK2D, Fig. 13B), the cAMP responsive element binding protein 1 (CREB1, Fig. 13C), and the CREB binding protein (CREBBP, Fig. 13D). Four genes were predictors of HIV and were also affected by HIV and cannabis interactions: Beclin 1 (BECN1, Fig. 13E), Plexin C1 (PLXNC1, Fig. 13F), survival of motor neuron 1 (SMN1, Fig. 13G), and the class II major histocompatibility complex molecule HLA-DRA (Fig. 13H). Four genes marked HIV- cannabis users and also significantly distinguished between HIV- and HIV+ cannabis users: the Protein Phosphatase 3 Catalytic Subunit Beta (PPP3CB, Fig. 13I) and subunit gamma (PPP3CC, Fig. 13J), the K-Ras gene (KRAS, Fig. 13K) and Cullin 2 (CUL2, Fig. 13L). Overall, there was a trend to regulation of gene transcription by cannabis in the context of HIV, but not in the uninfected group, further highlighting interaction effects.

**Table 3**  
Domain-specific Cognitive scores in HIV/CAN groups separated by METH status.

METH-	HIV-/CAN-	HIV-/CAN+	HIV+/CAN-	HIV+/CAN+	P value	Pairwise comparison
	1	2	3	4		
Global T	49.3 (7.2)	50.3 (6.0)	44.3 (5.0)	49.1 (5.6)	<b>0.055</b>	3 < 1*, 2*, 4
Verbal T	51.1 (10.3)	51.2 (7.0)	44.0 (7.8)	48.6 (10.0)	0.134	3 < 1*, 2
Executive Functions T	48.5 (9.0)	49.6 (8.2)	44.9 (6.7)	49.4 (7.4)	0.396	-
SIP T	48.8 (8.9)	49.2 (8.1)	47.2 (6.7)	49.2 (5.9)	0.880	-
Learning T	47.9 (8.8)	50.0 (6.8)	42.2 (8.0)	46.5 (6.8)	<b>0.089</b>	3 < 2*, 1
Memory T	48.0 (10.7)	50.4 (5.4)	41.0 (8.1)	50.2 (6.8)	<b>0.018</b>	3 < 1*, 2**, 4**
Attention/WM T	51.6 (10.8)	52.6 (12.2)	44.0 (7.5)	50.9 (10.1)	0.114	3 < 1*, 2*, 4
Motor T	49.9 (8.2)	50.5 (8.8)	43.4 (10.7)	48.9 (10.9)	0.213	3 < 1, 2

Note: listed in table, p < 0.10; \*p < 0.05; \*\*p < 0.01.

METH+	HIV-/CAN-	HIV-/CAN+	HIV+/CAN-	HIV+/CAN+	P value	PW comparison
	1	2	3	4		
Global T	44.2 (5.2)	47.8 (4.5)	47.0 (6.4)	45.3 (7.3)	0.443	-
Verbal T	47.1 (8.0)	50.3 (10.2)	50.2 (9.0)	46.9 (9.5)	0.660	-
Executive Functions T	43.1 (5.4)	46.7 (5.5)	45.3 (9.1)	45.0 (8.0)	0.674	-
SIP T	47.2 (9.7)	49.5 (6.4)	48.1 (12.0)	46.9 (6.9)	0.898	-
Learning T	39.9 (7.8)	44.4 (5.2)	44.6 (7.8)	41.8 (10.8)	0.403	-
Memory T	40.0 (8.9)	45.8 (8.8)	45.3 (7.4)	42.7 (9.7)	0.332	-
Attention/WM T	46.7 (8.3)	47.8 (10.0)	45.3 (8.6)	44.8 (8.1)	0.832	-
Motor T	42.7 (7.8)	47.0 (9.2)	49.7 (10.0)	46.4 (11.9)	0.264	1 < 3

Note: listed p < 0.10, \*p < 0.05.

**Table 4**  
Cohen's d effect sizes relative to the HIV+/CAN- group (METH- participants only).

	HIV-/CAN-	HIV-/CAN+	HIV+/CAN+
Global T	<b>-0.82</b>	<b>-1.11</b>	-0.92
Verbal T	-0.77	<b>-0.95</b>	-0.53
Executive Functions T	-0.46	-0.63	-0.64
SIP T	-0.21	-0.28	-0.32
Learning T	-0.68	<b>-1.02</b>	-0.56
Memory T	-0.73	<b>-1.32</b>	<b>-1.21</b>
Attention/WM T	<b>-0.82</b>	<b>-0.90</b>	<b>-0.81</b>
Motor T	-0.68	-0.70	-0.51

Note. Bolded = Large effect size (Cohen's d > 0.80).

### 3.5. Effects of polysubstance use comorbidities

We have weighted the impact of polysubstance use in relation to CAN in the context of HIV. Table 3 shows the domain scores by METH group indicating that the pattern we observed in terms of global cognition, that is, potential benefit of cannabis use on cognition in HIV+, is reduced in the context of other drug use (i.e., methamphetamine). When the four HIV/CAN groups are stratified by METH use (i.e., Lifetime METH Abuse/Dependence), we did not observe any significant differences across the HIV/CAN groups in the METH+ group, but in the METH- group, the pattern described above is observed globally, and across domains, with

the most prominent differences observed in the domains of memory and working memory, and the least differences for the speeded information processing domain, as shown by the calculation of effect sizes (Table 4).

Similarly, genes showing distinct patterns in mixed models with METH as a covariate highlight the challenges of biomarker research in the context of substance use disorders. The findings suggest that polysubstance use in HIV may explain variability and limit discovery power. The analysis of the effects of interaction between HIV and other drugs such as METH, alcohol and cocaine using mixed models has shown that these drugs further increase the expression of a number of biomarkers in the HIV+ group, but cannabis decreases these effects (Fig. 14). For instance, METH dependence in HIV+CAN- subjects, but not in HIV+CAN+, was associated with increased NPC2 (Fig. 14A), FYN (Fig. 14B) and TLR2 (Fig. 14D). METH use increased the expression of CAST in all groups, but not in HIV+CAN+ subjects (Fig. 14C). A similar effect was observed in the expression of Perforin 1 (PFN1) when alcohol dependence was tested as a co-variate (Fig. 14E), and in the expression of CD44 in cocaine users (Fig. 14F). Overall this indicates that cannabis is a strong confounder in biomarker associated with HIV, drug abuse and polysubstance use interactions.

On the other hand, although cannabis reverted the expression of markers that were elevated by HIV and METH, effects of cannabis on cognition were beneficial in non-METH users. Fig. 15 shows Global T scores, where higher values indicate better overall cognitive performance. In the context of METH-/CAN-, HIV+ participants performed worse; in the context of HIV-CAN-, METH+ participants perform worse overall. However, in the context of HIV+, cannabis users had better neurocognitive performance if they did not have a history of lifetime METH dependence. This suggests confounding effects of polysubstance use and that the potentially beneficial effect of cannabis on HIV biomarkers may be reduced when other drugs are used.

## 4. Discussion

The screening of a large number of transcripts associated with neurological disorders has shown that the effects of cannabis differed drastically between HIV- and HIV+ groups, particularly in gene networks playing a role in inflammation, neurodegeneration, apoptosis and leukocyte adhesion and transmigration. The results indicate that cannabis in the context of HIV may have beneficial effects. However, in individual genes, we identified detrimental effects that were associated with polysubstance use as a covariate, particularly methamphetamine.

Effects of cannabis, one of the most widely used drugs, on HIV and particularly on biomarkers of inflammation and cognition, are largely unknown, diverse or anecdotal. By examining a large number of transcripts associated with neurological disorders and pathways of inflammation in peripheral leukocytes, we fill a gap on the understanding of how drugs of abuse impact cellular phenotypes, with the goals of identifying biomarkers of HIV neurocognitive disorders that are sensitive to interactions with substance use. In this study, we examined cells from 102 subjects evenly distributed as HIV+/-and CAN+/. In order to increase the power, the cohort was homogeneous in sex, age and education. The use of other substances was limited but not excluded, due to characteristics of the population. The sample size was a limitation for the identification of strong predictors. However, systems biology strategies helped us identify genes that exhibited interactive properties based on their co-involvement in highly overlapping molecular pathways. Visualization strategies helped identify gene networks with a concerted behavior in different groups, highlighting important trends in effects of cannabis use dependence.

Our results show that cannabis has strong effects on the expression of a number of genes in peripheral leukocytes, which serve as reporters of biological processes that are relevant both to HIV infection as well as to neurological disorders. For instance, the pathway identified as viral host interactions included class II HLA-DRA, CCR5 and CCR2. While HIV in the context of cannabis developed to lower expression of HLA-DRA,

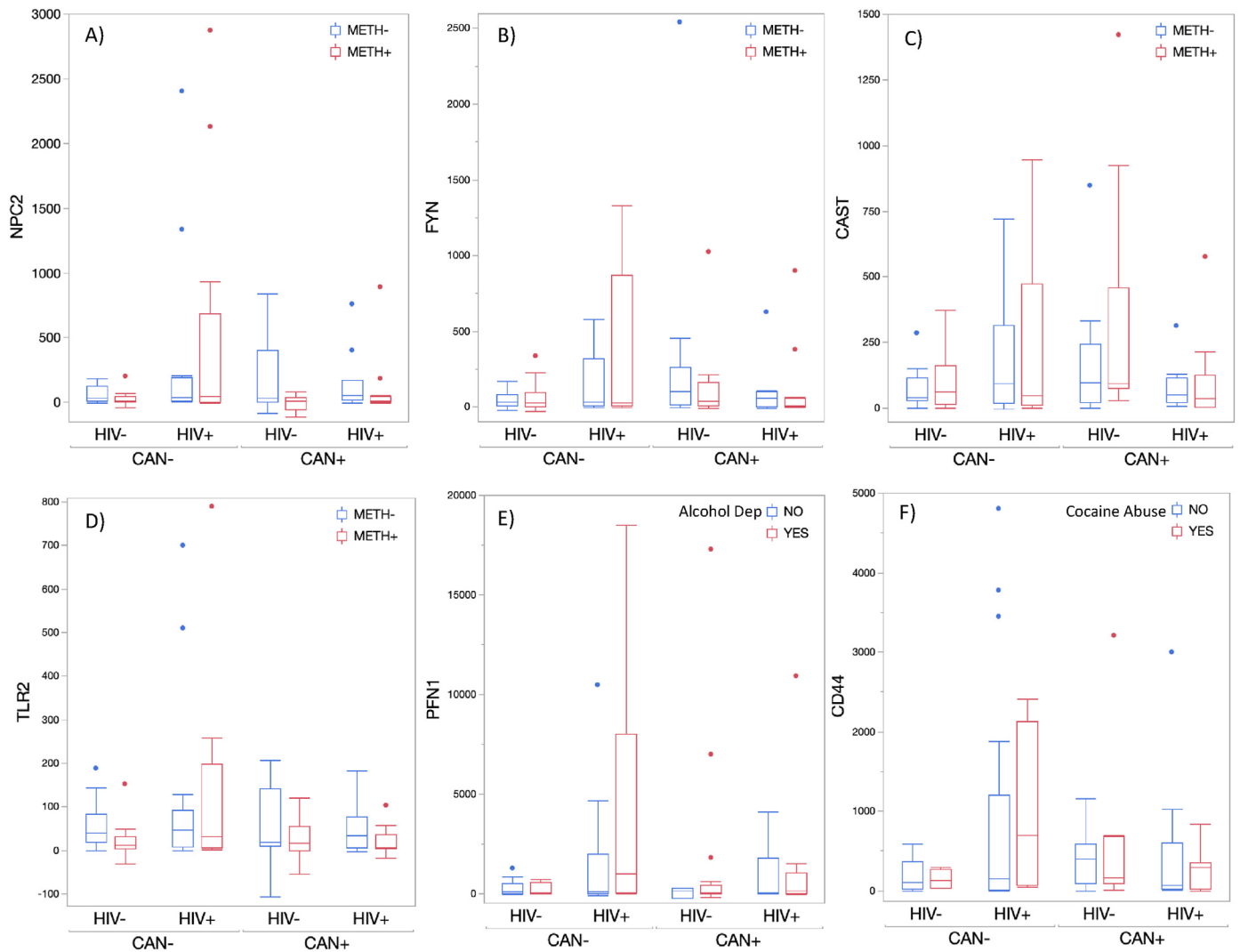


**Fig. 14.** Effects of cannabis on molecular biomarkers of HIV in the context of other substances. Transcripts that were influenced by HIV and other substances of abuse interactions and that were significantly decreased by cannabis. These transcripts were identified in mixed models followed by multiple comparisons. A) NPC2, B) FYN, C) CAST and D) TLR2 were influenced by Methamphetamine (METH). E) PFN1 was modified by alcohol dependence. F) CD44 was influenced by cocaine use.

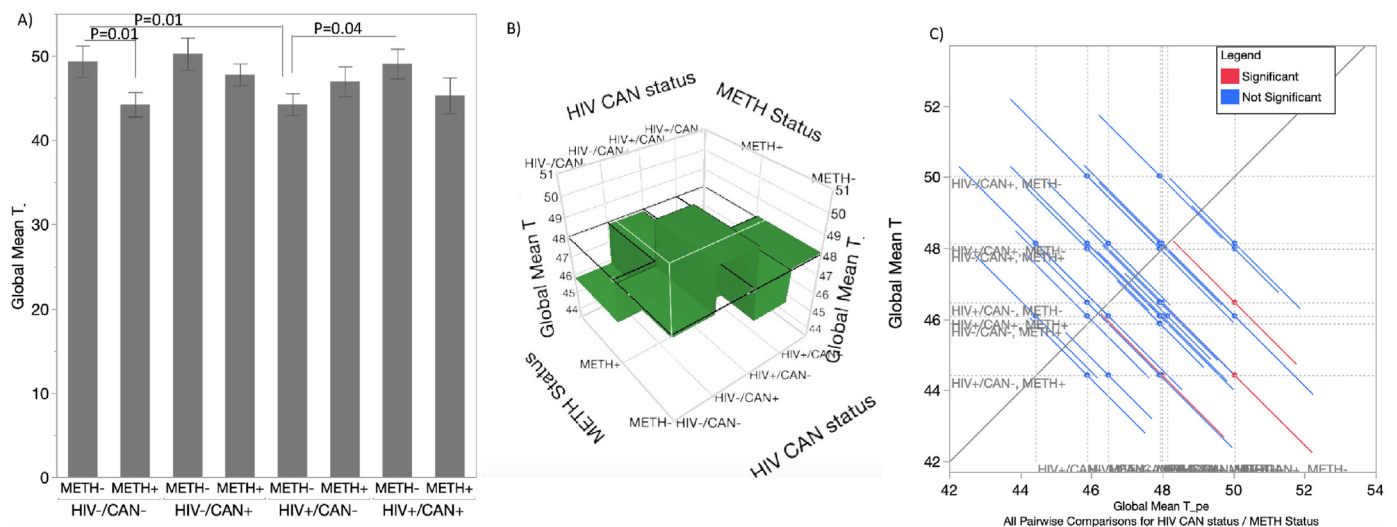


**Fig. 15.** Effects of cannabis and HIV on Global T scores and effects of METH as a co-variate. A) Neurobehavioral data as Global T scores was analyzed for covariate effects. P values from multiple comparisons are indicated. B) Marginal model interference surface profiler. C) Visualization of Global Mean T pairwise comparisons used to confirm significant differences.

cannabis did not lower the transcription of CCR5, suggesting a limited impact on viral entry (Lopalco, 2010). On the other hand, HIV in the context of cannabis and cannabis alone showed detectable decrease in the transcription of SIRT1, a histone deacetylase with epigenetic silencing properties (Bortell et al., 2018). We have previously reported that the transcriptional decrease of SIRT1 may be one factor in the dysregulation of the inflammatory environment (Bortell et al., 2018) and others have suggested that SIRT1 regulates viral transcription (Pagans et al., 2005; Zhang et al., 2009). Whether the effects of cannabis in this pathway have real implications to the infection remains to be addressed. In this cohort, we did not find correlations between the activation of these pathways in leukocytes and plasma or CSF viral load (not shown). Yet, the attenuating effects of cannabis observed in the context of HIV links and expands to pathways in inflammation and neurodegeneration, as well as to apoptosis, due to overlap in genes and transcriptional co-regulators (Zicari et al., 2019; Kaul et al., 2001; Kaul and Lipton, 2006).

The actions of cannabis on the expression of genes involved in vascular adhesion and leukocyte transmigration have indicated that in HIV+ cannabis users, peripheral leukocytes may be less likely to focally adhere to endothelial cells and migrate into tissues. This may be beneficial at preventing inflammation in end-organs including the brain, while potentially impairing surveillance, but also viral spread (Williams et al., 2012). The implications of this findings must be addressed using experimental models.

Overall, the findings were consistent across pathways, suggesting that, like HIV alone, cannabis alone may increase the expression of a number of inflammation-associated genes, but this may differ in the context of HIV, where cannabis use was associated with attenuated or decreased expression of pathway components. In end organs, the actions of cannabis may differ due to effects via distinct receptors. Cannabinoid receptor 1 (CB1R) is largely expressed in CNS but also in several tissues with links to psychoactive and physiological effects, while CB2R is expressed mainly by immune cells with described anti-inflammatory and immunosuppressive properties (Galiegue et al., 1995; Ashton and Glass, 2007; Graham et al., 2009). Given the differences in distribution and signaling between the receptors, effects of cannabis or cannabinoids may differ in the presence or absence of inflammatory cells, or in the context of infection, where pro-inflammatory signals are occurring. Other less studied cannabinoid receptors and endocannabinoids may also play a role. Our data supports this idea that cannabis effects on molecular markers and biological processes is context-dependent, potentially driven by infection and inflammation, and the resulting differences in numbers and activation status of CB2R-expressing innate and adaptive immune cells.

The examination of changes in expression patterns in kinase networks can inform mechanisms of action by cannabis in the context of HIV. Aberrant kinase activity is linked to a wide range of diseases including neoplastic diseases, central nervous system (CNS) disorders, vascular disorders, and chronic inflammatory diseases. The analysis of a gene networks assigned to kinases indicated that cannabis in the context of HIV decreased transcription of components of the p38 MAPK pathway, which is involved in a diversity of biological functions (Cuadrado and Nebreda, 2010). The blockage of p38 MAPK by cannabinoids has been previously reported in other models, with both suppressor and stimulating effects (El-Remessy et al., 2008; Herrera et al., 2005; Derkinderen et al., 2001). Suppression of this pathway may be associated with blockage of oxidative stress (Cuadrado and Nebreda, 2010; El-Remessy et al., 2008). The anti-oxidant activity of cannabis and cannabinoid compounds has been previously acknowledged (Raja et al., 2020; Abdel-Salam et al., 2012; Cassol et al., 2010), although healthy cannabis users do not differ from non-users regarding oxidative stress markers (Bayazit et al., 2017).

HIV infection promotes changes in the number of immune cells, quality and activation status of cell subsets. The infection and the broken homeostasis are likely critical in the determination of the effects of

cannabis as a therapy or a complication. It has been suggested that the effects of cannabinoids on macrophages are critical to resulting T-cell mediated responses and may differ according to those cells activation status and to stimuli (Chuchawankul et al., 2004). Moreover, here we have shown by transcription factor usage predictions, that the effects of cannabis are associated with transcriptional co-regulation at the individual gene promoters, by multiple factors that may vary by context. Co-regulation by different transcription factors is a critical factor in determination of transcriptional levels and kinetics (Kim et al., 2012; Sonda et al., 2011), and is highly influenced by covariates and comorbidities.

Cannabis use may be considered as a confounder in biomarker investigations as it tended to mask the expression of molecules upregulated by HIV, particularly if cognitive function was not improved in parallel with markers, for instance when other drugs were present. Cannabis users had better neurocognitive performance, overall and in learning and memory subdomains, particularly if they did not have a history of lifetime METH dependence. Such effect was stronger in METH users, but also observed in markers sensitive to HIV/alcohol and HIV/cocaine. This suggests differential effects of cannabis in the context of polysubstance use and how the potentially beneficial effect of cannabis on HIV biomarkers may be relative when other drugs are also used.

Overall, our work has screened effects of cannabis on an extensive number of transcript biomarkers of inflammation and neurological outcomes, which were peripherally expressed by uninfected and HIV-infected subjects. Systems biology strategies have aided the identification of gene networks assigned to processes relevant to neuroHIV, which exhibited orchestrated behaviors in response to HIV or cannabis alone, or their interactions. Cannabis effects were largely dependent on context, with infection as the most significant interacting factor followed by polysubstance use. Other factors not examined here may include cannabis use frequency and dose. The results suggest that cannabis may be beneficial in the context of HIV when other substances are not concomitantly used.

## Contributions

LVB prepared all the specimens for digital multiplexing, analyzed data and contributed to the manuscript; SEL performed systems biology analysis; RM advised on the choice of surface markers for flow cytometry, participated in all the discussions and contributed to the manuscript; RJE and MC selected the subjects in the cohort, participated in the design and discussions and contributed to the manuscript; JI contributed to the study design, to statistical decisions, participated in all the discussions and contributed to the manuscript; MCGM designed the study, prepared all the specimens for flow cytometry and RNA extraction, performed flow cytometry, analyzed the data, wrote the manuscript and obtained funding.

## Declaration of competing interest

The authors do not have any conflict of interest to declare.

## Acknowledgements

The authors want to thank Krista Scrivner and Christine Auciello for administrative assistance. This study was performed with funding from NIH R01DA047822 and CHRP H22BD4439 to MCGM. JI received funding from NIH R01DA053052, R01DA047879, and P30MH062512. The authors do not have any conflicts of interest.

## Appendix A. Supplementary data

Supplementary data to this article can be found online at <https://doi.org/10.1016/j.bbih.2022.100414>.



## References

- Abdel-Salam, O.M., El-Sayed El-Shamarka, M., Salem, N.A., El-Din, M.G.A., 2012. Effects of *Cannabis sativa* extract on haloperidol-induced catalepsy and oxidative stress in the mice. *EXCLI J* 11, 45–58. <https://doi.org/10.1016/j.excli.2012.01.001>. PubMed PMID: 237366134; PubMed Central PMCID: PMC34928014.
- Ashton, J.C., Glass, M., 2007. The cannabinoid CB2 receptor as a target for inflammation-dependent neurodegeneration. *Curr Neuropharmacol* 5 (2), 73–80. <https://doi.org/10.2174/157015907780866884>. Epub 2008/07/11, PubMed PMID: 18615177; PubMed Central PMCID: PMC2435344.
- Bachmann, N., von Siebenthal, C., Vongrad, V., Turk, T., Neumann, K., Beerenwinkel, N., et al., 2019. Determinants of HIV-1 reservoir size and long-term dynamics during suppressive ART. *Nat Commun* 10 (1), 3193. <https://doi.org/10.1038/s41467-019-10884-9>. Epub 2019/07/22, PubMed PMID: 31324762; PubMed Central PMCID: PMC6642170.
- Basova, L., Lindsey, A., McGovern, A.M., Ellis, R.J., Marcondes, M.C.G., 2021. Detection of H3K4me3 identifies NeuroHIV signatures, genomic effects of methamphetamine and addiction pathways in postmortem HIV+ brain specimens that are not amenable to transcriptome analysis. *Viruses* 13 (4). <https://doi.org/10.3390/v13040544>. Epub 2021/04/04, PubMed PMID: 33805201; PubMed Central PMCID: PMC8064323.
- Bayazit, H., Selek, S., Karababa, I.F., Cicek, E., Aksoy, N., 2017. Evaluation of oxidant/antioxidant status and cytokine levels in patients with cannabis use disorder. *Clin Psychopharmacol Neurosci* 15 (3), 237–242. <https://doi.org/10.9758/cpn.2017.15.3.237>. Epub 2017/08/09, PubMed PMID: 28783932; PubMed Central PMCID: PMC5565077.
- Blackstone, K., Moore, D.J., Franklin, D.R., Clifford, D.B., Collier, A.C., Marra, C.M., et al., 2012. Defining neurocognitive impairment in HIV: deficit scores versus clinical ratings. *Clin Neuropsychol* 26 (6), 894–908. <https://doi.org/10.1080/13804046.2012.694479>. Epub 2012/06/20, PubMed PMID: 22708483; PubMed Central PMCID: PMC348322.
- Bortell, N., Basova, L., Najera, J.A., Morsey, B., Fox, H.S., Marcondes, M.C.G., 2018. Sirtuin 1-chromatin-binding dynamics points to a common mechanism regulating inflammatory targets in SIV infection and in the aging brain. *J Neuroimmune Pharmacol* 13 (2), 163–178. <https://doi.org/10.1007/s11481-017-9772-3>. Epub 2017/12/28, PubMed PMID: 29280055; PubMed Central PMCID: PMC5930062.
- Brew, B.J., Barnes, S.L., 2019. The impact of HIV central nervous system persistence on pathogenesis. *AIDS* 33 (Suppl. 2), S113–S121. <https://doi.org/10.1097/QAD.0000000000002251>. Epub 2019/12/04, PubMed PMID: 31790377.
- Brew, B.J., McArthur, J., 2019. Distinguishing cognitive impairment from HIV-associated neurocognitive disorder versus substance use? *AIDS* 33 (12), 1943–1944. <https://doi.org/10.1097/QAD.0000000000002292>. Epub 2019/09/07, PubMed PMID: 31490213.
- Burdo, T.H., Katner, S.N., Taffe, M.A., Fox, H.S., 2006. Neuroimmunity, drugs of abuse, and neuroAIDS. *J Neuroimmune Pharmacol* 1 (1), 41–49. <https://doi.org/10.1007/s11481-005-9001-3>. Epub 2007/11/28, PubMed PMID: 18040790.
- Byrd, D.A., Fellows, R.P., Morgello, S., Franklin, D., Heaton, R.K., Deutsch, R., et al., 2011. Neurocognitive impact of substance use in HIV infection. *J Acquir Immune Defic Syndr* 58 (2), 154–162. <https://doi.org/10.1097/QAI.0b013e318229ba41>. Epub 2011/07/05, PubMed PMID: 21725250; PubMed Central PMCID: PMC3183737.
- Carey, C.L., Woods, S.P., Gonzalez, R., Conover, E., Marcotte, T.D., Grant, I., et al., 2004. Predictive validity of global deficit scores in detecting neuropsychological impairment in HIV infection. *J Clin Exp Neuropsychol* 26 (3), 307–319. <https://doi.org/10.1080/13803390490510031>. Epub 2004/10/30, PubMed PMID: 15512922.
- Cassol Jr., O.J., Comim, C.M., Silva, B.R., Hermani, F.V., Constantino, L.S., Felisberto, F., et al., 2010. Treatment with cannabidiol reverses oxidative stress parameters, cognitive impairment and mortality in rats submitted to sepsis by cecal ligation and puncture. *Brain Res* 1348, 128–138. <https://doi.org/10.1016/j.brainres.2010.06.023>. Epub 2010/06/22, PubMed PMID: 20561509.
- Chuchawankul, S., Shima, M., Buckley, N.E., Hartmann, C.B., McCoy, K.L., 2004. Role of cannabinoid receptors in inhibiting macrophage costimulatory activity. *Int Immunopharmacol* 4 (2), 265–278. <https://doi.org/10.1016/j.intimp.2003.12.011>. Epub 2004/03/05, PubMed PMID: 14996418.
- Cuadrado, A., Nebreda, A.R., 2010. Mechanisms and functions of p38 MAPK signalling. *Biochem J* 429 (3), 403–417. <https://doi.org/10.1042/BJ20100323>. Epub 2010/07/16, PubMed PMID: 20626350.
- Danaher, P., Warren, S., Dennis, L., D'Amico, L., White, A., Disis, M.L., et al., 2017. Gene expression markers of tumor infiltrating leukocytes. *J Immunother Cancer* 5, 18. <https://doi.org/10.1186/s40425-017-0215-8>. Epub 2017/02/28, PubMed PMID: 28239471; PubMed Central PMCID: PMC5319024.
- Derkinderen, P., Ledent, C., Parmentier, M., Girault, J.A., 2001. Cannabinoids activate p38 mitogen-activated protein kinases through CB1 receptors in hippocampus. *J Neurochem* 77 (3), 957–960. <https://doi.org/10.1046/j.1471-4159.2001.00333.x>. Epub 2001/05/02, PubMed PMID: 11331425.
- El-Remessy, A.B., Tang, Y., Zhu, G., Matragoon, S., Khalifa, Y., Liu, E.K., et al., 2008. Neuroprotective effects of cannabidiol in endotoxin-induced uveitis: critical role of p38 MAPK activation. *Mol Vis* 14, 2190–2203. Epub 2008/12/05. PubMed PMID: 19052649; PubMed Central PMCID: PMC2592995.
- Ellis, R.J., Peterson, S.N., Li, Y., Schrier, R., Iudicello, J., Letendre, S., et al., 2020. Recent cannabis use in HIV is associated with reduced inflammatory markers in CSF and blood. *Neurol Neuroimmunol Neuroinflamm* 7 (5). <https://doi.org/10.1212/NXI.0000000000000809>. Epub 2020/06/20, PubMed PMID: 32554630; PubMed Central PMCID: PMC7309527.
- Ferris, M.J., Mactutus, C.F., Booze, R.M., 2008. Neurotoxic profiles of HIV, psychostimulant drugs of abuse, and their concerted effect on the brain: current status of dopamine system vulnerability in NeuroAIDS. *Neurosci Biobehav Rev* 32 (5), 883–909. <https://doi.org/10.1016/j.neubiorev.2008.01.004>. Epub 2008/04/24, PubMed PMID: 18430470; PubMed Central PMCID: PMC2527205.
- Franz, M., Rodriguez, H., Lopes, C., Zuberi, K., Montojo, J., Bader, G.D., et al., 2018. GeneMANIA update 2018. *Nucleic Acids Res* 46 (W1), W60–W64. <https://doi.org/10.1093/nar/gky311>. Epub 2018/06/19, PubMed PMID: 29912392; PubMed Central PMCID: PMC6030815.
- Galiegue, S., Mary, S., Marchand, J., Dussossoy, D., Carriere, D., Carayon, P., et al., 1995. Expression of central and peripheral cannabinoid receptors in human immune tissues and leukocyte subpopulations. *Eur J Biochem* 232 (1), 54–61. <https://doi.org/10.1111/j.1432-1033.1995.tb20780.x>. Epub 1995/08/15, PubMed PMID: 7556170.
- Gama, L., Abreu, C.M., Shirk, E.N., Price, S.L., Li, M., Laird, G.M., et al., 2017. Reactivation of simian immunodeficiency virus reservoirs in the brain of virally suppressed macaques. *AIDS* 31 (1), 5–14. <https://doi.org/10.1097/QAD.0000000000001267>. Epub 2016/11/30, PubMed PMID: 27898590; PubMed Central PMCID: PMC55131686.
- Gonzalez, R., Rippeth, J.D., Carey, C.L., Heaton, R.K., Moore, D.J., Schweinsburg, B.C., et al., 2004. Neurocognitive performance of methamphetamine users discordant for history of marijuana exposure. *Drug Alcohol Depend* 76 (2), 181–190. <https://doi.org/10.1016/j.drugalcdep.2004.04.014>. Epub 2004/10/19, PubMed PMID: 15488342.
- Graham, E.S., Ashton, J.C., Glass, M., 2009. Cannabinoid Receptors: a brief history and what not. *Front Biosci (Landmark Ed)* 14, 944–957. <https://doi.org/10.2741/3288>. Epub 2009/03/11, PubMed PMID: 19273110.
- Grant, I., Gonzalez, R., Carey, C.L., Natarajan, L., Wolfson, T., 2003. Non-acute (residual) neurocognitive effects of cannabis use: a meta-analytic study. *J Int Neuropsychol Soc* 9 (5), 679–689. <https://doi.org/10.1017/S1355617703950016>. Epub 2003/08/07, PubMed PMID: 12901774.
- Haw, R.A., Croft, D., Yung, C.K., Ndegwa, N., D'Eustachio, P., Hermjakob, H., et al., 2011. The Reactome bioMart. Database (Oxford). <https://doi.org/10.1093/database/bar031>, 2011.bar031. Epub 2011/10/21, PubMed PMID: 22012987; PubMed Central PMCID: PMC3197281.
- Heaton, R.K.T.M., Manly, J.J., 2002. Demographic Effects and Use of Demographically Corrected Norms with the WAIS-III and WMS-III.
- Heaton, R.K.M.S., Taylor, M., 2004. Grant I Revised Comprehensive Norms for an Expanded Halstead-Reitan Battery: Demographically Adjusted Neuropsychological Norms for African American and Caucasian Adults Scoring Program. Psychological Assessment Resources, Lutz.
- Heaton, R.K., Franklin Jr., D.R., Deutsch, R., Letendre, S., Ellis, R.J., Casetto, K., et al., 2015. Neurocognitive change in the era of HIV combination antiretroviral therapy: the longitudinal CHARTER study. *Clin Infect Dis* 60 (3), 473–480. <https://doi.org/10.1093/cid/ciu862>. Epub 2014/11/02, PubMed PMID: 25362201; PubMed Central PMCID: PMC4303775.
- Herrera, B., Carracedo, A., Diez-Zaera, M., Guzman, M., Velasco, G., 2005. p38 MAPK is involved in CB2 receptor-induced apoptosis of human leukaemia cells. *FEBS Lett* 579 (22), 5084–5088. <https://doi.org/10.1016/j.febslet.2005.08.021>. Epub 2005/09/06, PubMed PMID: 16139274.
- Hunt, P.W., Lee, S.A., Siedner, M.J., 2016. Immune-inflammatory biomarkers, morbidity, and mortality in treated HIV infection. *J Infect Dis* 214 (Suppl. 2), S44–S50. <https://doi.org/10.1093/infdis/jiw275>. Epub 2016/09/15, PubMed PMID: 27625430; PubMed Central PMCID: PMC5021241.
- Kaul, M., Lipton, S.A., 2006. Mechanisms of neuronal injury and death in HIV-1 associated dementia. *Curr HIV Res* 4 (3), 307–318. <https://doi.org/10.2174/15701620677709384>. Epub 2006/07/18, PubMed PMID: 16842083.
- Kaul, M., Garden, G.A., Lipton, S.A., 2001. Pathways to neuronal injury and apoptosis in HIV-associated dementia. *Nature* 410 (6831), 988–994. <https://doi.org/10.1038/35073667>. Epub 2001/04/20, PubMed PMID: 11309629.
- Kim, J., Choi, M., Kim, J.R., Jin, H., Kim, V.N., Cho, K.H., 2012. The co-regulation mechanism of transcription factors in the human gene regulatory network. *Nucleic Acids Res* 40 (18), 8849–8861. <https://doi.org/10.1093/nar/gks664>. Epub 2012/07/17, PubMed PMID: 22798495; PubMed Central PMCID: PMC3467061.
- Koob, G.F., Volkow, N.D., 2016. Neurobiology of addiction: a neurocircuitry analysis. *Lancet Psychiatry* 3 (8), 760–773. [https://doi.org/10.1016/S2215-0366\(16\)00104-8](https://doi.org/10.1016/S2215-0366(16)00104-8). Epub 2016/08/01, PubMed PMID: 27475769; PubMed Central PMCID: PMC46135092.
- Lopalco, L., 2010. CCR5: from natural resistance to a new anti-HIV strategy. *Viruses* 2 (2), 574–600. <https://doi.org/10.3390/v2020574>. Epub 2010/02/01, PubMed PMID: 21994649; PubMed Central PMCID: PMC3185609.
- Lucey, D.R., Hensley, R.E., Ward, W.W., Butzin, C.A., Boswell, R.N., 1988. CD4+ monocyte counts in persons with HIV-1 infection: an early increase is followed by a progressive decline. *J Acquir Immune Defic Syndr* 4 (1), 24–30, 1991. Epub 1991/01/01. PubMed PMID: 1670587.
- Magrone, T., Jirillo, E., 2019. Drugs of abuse induced-subversion of the peripheral immune response and central glial activity: focus on novel therapeutic approaches. *Endocr Metab Immune Disord Drug Targets* 19 (3), 281–291. <https://doi.org/10.2174/1871530319666181129104329>. Epub 2018/11/30, PubMed PMID: 30488804.
- Marcondes, M.C., Flynn, C., Huitron-Rezendiz, S., Watry, D.D., Zandonati, M., Fox, H.S., 2009. Early antiretroviral treatment prevents the development of central nervous system abnormalities in simian immunodeficiency virus-infected rhesus monkeys. *AIDS* 23 (10), 1187–1195. <https://doi.org/10.1097/QAD.0b013e32832c4af0>. Epub 2009/05/21, PubMed PMID: 19455015; PubMed Central PMCID: PMC2698130.
- Montojo, J., Zuberi, K., Rodriguez, H., Kazi, F., Wright, G., Donaldson, S.L., et al., 2010. GeneMANIA Cytoscape plugin: fast gene function predictions on the desktop. *Bioinformatics* 26 (22), 2927–2928. <https://doi.org/10.1093/bioinformatics/btq562>. Epub 2010/10/12, PubMed PMID: 20926419; PubMed Central PMCID: PMC2971582.

- Montejo, J., Zuberi, K., Rodriguez, H., Bader, G.D., Morris, Q., 2014a. GeneMANIA: fast gene network construction and function prediction for Cytoscape. *F1000Res* 3, 153. <https://doi.org/10.12688/f1000research.4572.1>. Epub 2014/09/26, PubMed PMID: 25254104; PubMed Central PMCID: PMCPCMC4168749.
- Montejo, J., Zuberi, K., Shao, Q., Bader, G.D., Morris, Q., 2014b. Network Assessor: an automated method for quantitative assessment of a network's potential for gene function prediction. *Front Genet* 5, 123. <https://doi.org/10.3389/fgene.2014.00123>. Epub 2014/06/07, PubMed PMID: 24904632; PubMed Central PMCID: PMCPCMC4032932.
- Norman, M.A., Moore, D.J., Taylor, M., Franklin Jr., D., Cysique, L., Ake, C., et al., 2011. Demographically corrected norms for african Americans and caucasians on the Hopkins verbal learning test-revised, brief visuospatial memory test-revised, Stroop color and Word test, and Wisconsin card sorting test 64-card version. *J Clin Exp Neuropsychol* 33 (7), 793–804. <https://doi.org/10.1080/13803395.2011.559157>. Epub 2011/05/07, PubMed PMID: 21547817; PubMed Central PMCID: PMCPCMC3154384.
- Oughtred, R., Rust, J., Chang, C., Breitkreutz, B.J., Stark, C., Willems, A., et al., 2021. The BioGRID database: a comprehensive biomedical resource of curated protein, genetic, and chemical interactions. *Protein Sci* 30 (1), 187–200. <https://doi.org/10.1002/pro.3978>. Epub 2020/10/19, PubMed PMID: 33070389; PubMed Central PMCID: PMCPCMC7737760.
- Pagans, S., Pedal, A., North, B.J., Kaehlcke, K., Marshall, B.L., Dorr, A., et al., 2005. SIRT1 regulates HIV transcription via Tat deacetylation. *PLoS Biol* 3 (2), e41. <https://doi.org/10.1371/journal.pbio.0030041>. Epub 2005/02/19, PubMed PMID: 15719057; PubMed Central PMCID: PMCPCMC546329.
- Paolillo, E.W., Pasipanodya, E.C., Moore, R.C., Pence, B.W., Atkinson, J.H., Grelotti, D.J., et al., 2020. Cumulative burden of depression and neurocognitive decline among persons with HIV: a longitudinal study. *J Acquir Immune Defic Syndr* 84 (3), 304–312. <https://doi.org/10.1097/QAI.0000000000002346>. Epub 2020/03/21, PubMed PMID: 32195746.
- Raja, A., Ahmadi, S., de Costa, F., Li, N., Kerman, K., 2020. Attenuation of oxidative stress by cannabinoids and cannabis extracts in differentiated neuronal cells. *Pharmaceuticals (Basel)* 13 (11). <https://doi.org/10.3390/ph13110328>. Epub 2020/10/28, PubMed PMID: 33105840; PubMed Central PMCID: PMCPCMC7690570.
- Rizzo, M.D., Crawford, R.B., Henriquez, J.E., Aldhamen, Y.A., Gulick, P., Amalfitano, A., et al., 2018. HIV-infected cannabis users have lower circulating CD16+ monocytes and IFN-gamma-inducible protein 10 levels compared with nonusing HIV patients. *AIDS* 32 (4), 419–429. <https://doi.org/10.1097/QAD.0000000000001704>. Epub 2017/12/02, PubMed PMID: 29194121; PubMed Central PMCID: PMCPCMC5790621.
- Saloner, R., Fields, J.A., Marcondes, M.C.G., Iudicello, J.E., von Kanel, S., Cherner, M., et al., 2020. Methamphetamine and cannabis: a tale of two drugs and their effects on HIV, brain, and behavior. *J Neuroimmune Pharmacol* 15 (4), 743–764. <https://doi.org/10.1007/s11481-020-09957-0>. Epub 2020/09/16, PubMed PMID: 32929575; PubMed Central PMCID: PMCPCMC7719083.
- Saloner, R., Paolillo, E.W., Heaton, R.K., Grelotti, D.J., Stein, M.B., Miller, A.H., et al., 2021. Chronically elevated depressive symptoms interact with acute increases in inflammation to predict worse neurocognition among people with HIV. *J Neurovirol* 27 (1), 160–167. <https://doi.org/10.1007/s13365-020-00925-1>. Epub 2021/01/07, PubMed PMID: 33405198.
- Shannon, P., Markiel, A., Ozier, O., Baliga, N.S., Wang, J.T., Ramage, D., et al., 2003. Cytoscape: a software environment for integrated models of biomolecular interaction networks. *Genome Res* 13 (11), 2498–2504. <https://doi.org/10.1101/gr.1239303>. Epub 2003/11/05, PubMed PMID: 14597658; PubMed Central PMCID: PMCPCMC403769.
- Sonda, N., Chioda, M., Zilio, S., Simonato, F., Bronte, V., 2011. Transcription factors in myeloid-derived suppressor cell recruitment and function. *Curr Opin Immunol* 23 (2), 279–285. <https://doi.org/10.1016/j.coi.2010.12.006>. Epub 2011/01/14, PubMed PMID: 21227670.
- Stark, C., Breitkreutz, B.J., Reguly, T., Boucher, L., Breitkreutz, A., Tyers, M., 2006. BioGRID: a general repository for interaction datasets. *Database issue Nucleic Acids Res* 34, D535–D539. <https://doi.org/10.1093/nar/gkj109>. Epub 2005/12/31, PubMed PMID: 16381927; PubMed Central PMCID: PMCPCMC1347471.
- Stein, L.D., 2004. Using the reactome database. *Curr Protoc Bioinformatics*. <https://doi.org/10.1002/0471250953.bi0807s7>. Chapter 8:Unit 8 7. Epub 2008/04/23, PubMed PMID: 18428737.
- Tjitro, R., Campbell, L.A., Basova, L., Johnson, J., Najera, J.A., Lindsey, A., et al., 2018. Modeling the function of TATA box binding protein in transcriptional changes induced by HIV-1 Tat in innate immune cells and the effect of methamphetamine exposure. *Front Immunol* 9, 3110. <https://doi.org/10.3389/fimmu.2018.03110>. Epub 2019/02/20, PubMed PMID: 30778358; PubMed Central PMCID: PMCPCMC6369711.
- Veenstra, M., Leon-Rivera, R., Li, M., Gama, L., Clements, J.E., Berman, J.W., 2017. Mechanisms of CNS viral seeding by HIV(+) CD14(+) CD16(+) monocytes: establishment and reseeding of viral reservoirs contributing to HIV-associated neurocognitive disorders. *mBio* 8 (5). <https://doi.org/10.1128/mBio.01280-17>. Epub 2017/10/27, PubMed PMID: 29066542; PubMed Central PMCID: PMCPCMC5654927.
- Volkow, N.D., Morales, M., 2015. The brain on drugs: from reward to addiction. *Cell* 162 (4), 712–725. <https://doi.org/10.1016/j.cell.2015.07.046>. Epub 2015/08/16, PubMed PMID: 26276628.
- Wallet, C., De Rovere, M., Van Assche, J., Daouad, F., De Wit, S., Gautier, V., et al., 2019. Microglial cells: the main HIV-1 reservoir in the brain. *Front Cell Infect Microbiol* 9, 362. <https://doi.org/10.3389/fcimb.2019.00362>. Epub 2019/11/12, PubMed PMID: 31709195; PubMed Central PMCID: PMCPCMC6821723.
- Warde-Farley, D., Donaldson, S.L., Comes, O., Zuberi, K., Badrawi, R., Chao, P., et al., 2010. The GeneMANIA prediction server: biological network integration for gene prioritization and predicting gene function. *Web Server issue Nucleic Acids Res* 38, W214–W220. <https://doi.org/10.1093/nar/gkq537>. Epub 2010/07/02, PubMed PMID: 20576703; PubMed Central PMCID: PMCPCMC2896186.
- Watson, C.W., Paolillo, E.W., Morgan, E.E., Umlauf, A., Sundermann, E.E., Ellis, R.J., et al., 2020. Cannabis exposure is associated with a lower likelihood of neurocognitive impairment in people living with HIV. *J Acquir Immune Defic Syndr* 83 (1), 56–64. <https://doi.org/10.1097/QAI.0000000000002211>. Epub 2019/12/07, PubMed PMID: 31809361; PubMed Central PMCID: PMCPCMC6901104.
- Whiting, P.F., Wolff, R.F., Deshpande, S., Di Nisio, M., Duffy, S., Hernandez, A.V., et al., 2015. Cannabinoids for medical use: a systematic review and meta-analysis. *JAMA* 313 (24), 2456–2473. <https://doi.org/10.1001/jama.2015.6358>. Epub 2015/06/24, PubMed PMID: 26103030.
- Williams, D.W., Eugenin, E.A., Calderon, T.M., Berman, J.W., 2012. Monocyte maturation, HIV susceptibility, and transmigration across the blood brain barrier are critical in HIV neuropathogenesis. *J Leukoc Biol* 91 (3), 401–415. <https://doi.org/10.1189/jlb.0811394>. Epub 2012/01/10, PubMed PMID: 22227964; PubMed Central PMCID: PMCPCMC3289493.
- Wong, M.E., Jaworowski, A., Hearn, A.C., 2019. The HIV reservoir in monocytes and macrophages. *Front Immunol* 10, 1435. <https://doi.org/10.3389/fimmu.2019.01435>. Epub 2019/07/13, PubMed PMID: 31297114; PubMed Central PMCID: PMCPCMC6607932.
- Yuan, N.Y., Kaul, M., 2021. Beneficial and adverse effects of cART affect neurocognitive function in HIV-1 infection: balancing viral suppression against neuronal stress and injury. *J Neuroimmune Pharmacol* 16 (1), 90–112. <https://doi.org/10.1007/s11481-019-09868-9>. Epub 2019/08/07, PubMed PMID: 31385157; PubMed Central PMCID: PMCPCMC7233291.
- Zhang, H.S., Zhou, Y., Wu, M.R., Zhou, H.S., Xu, F., 2009. Resveratrol inhibited Tat-induced HIV-1 LTR transactivation via NAD(+)-dependent SIRT1 activity. *Life Sci* 85 (13–14), 484–489. <https://doi.org/10.1016/j.lfs.2009.07.014>. Epub 2009/08/12, PubMed PMID: 19664641.
- Zicari, S., Sessa, L., Cotugno, N., Ruggiero, A., Morrocchi, E., Concato, C., et al., 2019. Immune activation, inflammation, and non-AIDS Co-morbidities in HIV-infected patients under long-term ART. *Viruses* 11 (3). <https://doi.org/10.3390/v11030200>. Epub 2019/03/02, PubMed PMID: 30818749; PubMed Central PMCID: PMCPCMC6466530.